Thermochimica Acta, 17 (1976) 29–63

THE KINETICS OF TOBACCO PYROLYSIS

RICHARD R. BAKER

Group Research and Development Centre, British-American Tobacco Co. Ltd., Regent's Park Road, Southampton SO9 1PE, (England)

(Received 17 February 1976)

ABSTRACT

When tobacco is pyrolysed under non-isothermal flow conditions in an inert atmosphere, variation of the inert gas or its space velocity has only a minor effect on the profiles of formation rate versus temperature for seven product gases. Thus, mass transfer processes between the tobacco surface and the gas phase are very rapid, and the products are formed at an overall rate which is determined entirely by that of the chemical reactions.

The effect of radical chain inhibitors (nitrogen oxides) on the pyrolysis is complex because of the resultant oxidation. Nevertheless, no evidence was found for the occurrence of radical chain reactions in the gas phase. A small proportion (less than 10%) of all the gases monitored are formed by homogeneous decomposition of volatile and semi-volatile intermediate products, in the furnace used.

At temperatures above about 600°C the reduction of carbon dioxide to carbon monoxide by the carbonaceous tobacco residue becomes increasingly important. However, when tobacco is pyrolysed in an inert atmosphere, only a small amount of carbon dioxide is produced above 600°C and consequently its reduction to carbon monoxide contributes only a small proportion to the total carbon monoxide formed above that temperature. The rate of the tobacco/carbon dioxide reaction is controlled by chemical kinetic rather than mass transfer effects. Carbon monoxide reacts with tobacco to a small extent.

When the tobacco is pyrolysed in an atmosphere containing oxygen (9–21% v/v), some oxidation occurs at 200°C. At 250°C the combustion rate is controlled jointly by both kinetic and mass transfer processes, but mass transfer of oxygen in the gas phase becomes increasingly important as the temperature is increased, and it is dominant above 400°C. About 8% of the total carbon monoxide formed by combustion is lost by its further oxidation.

The results imply that *inside* the combustion coal of a burning cigarette the actual reactions occurring are of secondary importance, the rate of supply of oxygen being the dominant factor in determining the combustion rate and heat generation. In contrast, in the region immediately *behind* the coal, where a large proportion of the products which enter mainstream smoke are formed by thermal decomposition of tobacco constituents, the chemistry of the tobacco substrate is critical, since the decomposition kinetics are controlled by chemical rather than mass transfer effects.

INTRODUCTION

The interior of the combustion coal of a burning cigarette is oxygen deficient[1,2]. Carbon monoxide and dioxide present in the smoke are produced by both combustion and thermal decomposition of the tobacco[3,4].

Previous studies have confirmed that both oxides of carbon can be formed from the thermal decomposition of tobacco[2,5–7]. When flue-cured tobacco is heated at 1 to 12 K sec^{-1} in an inert atmosphere under flow conditions, 27% of the carbon content of the tobacco is converted to carbon oxides[6]. Both oxides show two distinct formation regions: a low-temperature region (about 100–450°C), and a high-temperature region (about 550–900°C).

Under oxidation conditions, about 70% of both carbon oxides formed in the low-temperature region are produced by tobacco decomposition reactions, whereas in the high-temperature region about 10–20% of the carbon monoxide and 2–9% of the carbon dioxide, are produced by tobacco decomposition.

Many aspects of the mechanism of the formation of gases from tobacco pyrolysis are unknown, in particular the contributions from radical reactions, heterogeneous and homogeneous reactions, reaction of intermediate products and the effect of mass transfer processes on the gas formation rates. For the present study, an automated pyrolysis technique with a data collection procedure and off-line computer processing of the results has been developed. Using these methods, aspects of the mechanism can be systematically assessed.

EXPERIMENTAL

Pyrolysis system

The pyrolysis experiments were carried out under non-isothermal flow conditions, and the cylindrical furnace (8 mm i.d., 220 mm long) was similar to that described previously[6]. Usually, 1 g of tobacco was placed in the furnace, the inlet gas flow was kept constant, and the material flowing out of the furnace was filtered by passing through two Cambridge filters* in series. A small part of the flow of filtered gases (0.08 cm^3 sec^{-1}) went into the capillary tube of the direct inlet system to a Finnigan 400 quadrupole mass spectrometer. The remainder of the gases flowed past an Ether pressure transducer (Type UP1) for measurement of the total gas flow-rate. Finally, the gases flowed directly into the detection cell of a Bosch infrared analyser (Type EFAW 215) for measurement of the carbon monoxide content.

The mass spectrometer was used in conjunction with an eight-channel peak selector (Finnigan Model 400-280-02) which scanned eight selected peaks in the mass spectrum of the pyrolysis gases at a scan rate of 7.5 msec per channel, and gave a quasi-continuous output for the intensity of each selected peak. These eight outputs,

*58 mm diameter, 1.4 mm thick filter disc made of interwoven glass fibres by Cambridge Filter Corporation, Syracuse, New York. The filter traps the aerosol particles in cigarette smoke.

together with the output from the ionisation gauge (Edwards Model IG5M) which measures the pressure in the ionisation chamber of the mass spectrometer, and the outputs from the thermocouple* inside the tobacco sample, the Bosch infrared analyser, and the pressure transducer, were monitored on a multichannel data logging system. The latter system consisted of CAMAC data-handling modules, manufactured by Nuclear Enterprises Ltd. Thus, a total of twelve channels of the data logger monitored twelve inputs from the experimental system.

Experimental procedure

For a given set of experimental parameters, a total of four replicate experiments were performed: two replicate experiments with the thermocouple at the linear and radial centre of the tobacco, and two with the thermocouple at the linear centre of the tobacco, and 1 mm from the furnace wall (the cylindrical furnace had an i.d. of 8 mm and the tobacco sample extended right across the furnace diameter). The pressure transducer and gas analysers were systematically calibrated immediately before each replicate experiment, using known gas mixtures and flow-rates.

During the pyrolysis the furnace was heated from room temperature to about 1000°C. The CAMAC data logging system scanned its input data at pre-set time intervals (dependent on the heating rate applied to the tobacco). The calibration and experimental data from the four replicates, obtained on punched paper tape from the CAMAC data logger, were processed on an off-line computer.

Data processing

Preliminary calibration experiments showed that for all the gases determined by mass spectrometry, the peak intensity/gas concentration relationships were linear. The pressure transducer output/volumetric gas flow relationship was also linear. The infrared analyser output/carbon monoxide concentration and thermocouple e.m.f./temperature relationships were quadratic.

The peaks monitored in the low resolution mass spectrum of the pyrolysis gases were $m/e = 2$, 14, 16, 30, 32, 42, 43 and 44. Many of these peaks consist of contributions from more than one component**. The peaks at m/e values 2, 32 and 44 can accurately be used to monitor hydrogen, oxygen, and carbon dioxide, respectively, the maximum contributions from other components in the pyrolysis gases being less than 1% in all cases. The peaks at m/e values 30 and 43 were used uncorrected to obtain the concentrations of ethane and propane, respectively, and the resultant concentrations may be too high by up to 10 and 25%, respectively, due to contributions from other species in the pyrolysis gases[2]. The concentrations of methane,

*A Pt/Pt–13% Rh thermocouple (0.05 mm diameter wire), used in conjunction with a cold junction compensation unit (manufactured by Nuclear Enterprises Ltd.).

**In particular, $m/e = 16$ is due to CH_4^+ (from methane) and O^+, O_2^{2+} (from oxygen, carbon monoxide and carbon dioxide); $m/e = 14$ is due to N^+, N_2^{2+} (from nitrogen), CH_2^+ (from hydrocarbons), and CO^{2+} (from carbon monoxide and dioxide); while $m/e = 42$ is due to, inter alia, $C_3H_6^+$ (from propane and propene).

propene, and nitrogen were obtained by solving the simultaneous equations for concentration and intensities of the multi-component peaks, as described previously[2].

Thus the appropriate experimental data values on the punched paper tape from each pyrolysis were converted on a computer to temperature (°C), rate of temperature increase (K sec^{-1}), total gas flow (cm^3 sec^{-1}), pressure inside the mass spectrometer (μtorr), and concentration of individual gases (% v/v). The rate of formation of a given gas (μmol sec^{-1}) was calculated assuming ideal behaviour of the flowing gases, using the total gas flow and concentration of individual gas, as described previously[6].

The mean of the two replicates of central and side tobacco temperature, and the four replicates of the rates of formation of the various gases together with the variation at the 95% confidence limit, were calculated at each time interval during the pyrolysis. The total amount of individual products formed for various extents of reaction were calculated. Finally, the computer program plotted the central and side tobacco temperature against reaction time, and the rate of formation of the gases against mean tobacco temperature.

PART 1. FACTORS AFFECTING THE PYROLYSIS OF TOBACCO IN THE ABSENCE OF OXYGEN

Results

The products monitored from the pyrolysis of flue-cured Virginia tobacco were hydrogen, methane, ethane, propane, propene, carbon monoxide and carbon dioxide. The shapes of the gas formation rate/temperatures profiles for carbon monoxide and dioxide are identical to those obtained previously using an A.E.I. MS2 mass spectrometer[6]. The profiles for methane, propane, and the carbon oxides, are similar to those obtained by Burton[7] using University of Kentucky IRI reference blend tobacco pyrolysed in helium at 0.1 K sec^{-1}, with products analysed chromatographically. However, the profile shapes for ethane and propane are significantly different to those reported by Burton, presumably caused by differences in the two tobacco compositions.

The 95% confidence limits of the points on the formation rate profiles are dependent on the magnitude of the quantity being analysed. The confidence limit of the carbon monoxide formation rate points is 2–10% of the formation rate value; that of the hydrogen and carbon dioxide points is 5–10%; methane is 10–20%; propane is 8–25%; ethane is 15–30%; while that of propene is 15–35%.

Although small amounts of molecular nitrogen are produced by a burning cigarette[8], distinct nitrogen profiles amongst the background scatter of the corrected $m/e = 14$ peak were not observed in the present study. This is entirely due to the relatively small contribution of nitrogen to that peak.

1.1 The effect of homogeneous reaction of intermediate products

The residence time in the furnace was varied for the pyrolysis products from tobacco heated in argon, in order to assess the contribution of homogeneous reaction of these products to the overall production rates of the gases. Two experiments were

carried out: one in which 0.25 g tobacco was pyrolysed near the furnace inlet, such that the pyrolysis products flowed for 200 mm through the heated zone before leaving the furnace; in the second experiment 0.25 g of tobacco was pyrolysed near the furnace exit, and the pyrolysis products travelled 20 mm before leaving the furnace. The residence time in the furnace depended on the rate of production of gases (i.e., total flow in the furnace) and the furnace temperature. With the tobacco at the furnace inlet position, the residence time decreased from 3.0 sec at room temperature to 0.7 sec at 1000°C (flow of argon into the furnace = 3.33 cm^3 sec^{-1}). The residence times for the "inlet" experiment were ten times longer than those for the "exit" experiment.

For all the gases determined, the rate of formation was greater in the" inlet" experiment up to at least 800°C. The formation profile for propane, for example, is shown in Fig. 1 and the total quantities of gases formed are summarised in Table 1*.

During the course of the whole pyrolysis, the rate of production of all gases increases as the residence time of the pyrolysis products in the furnace increases. Thus a proportion of all the gases monitored are formed by homogeneous decomposition

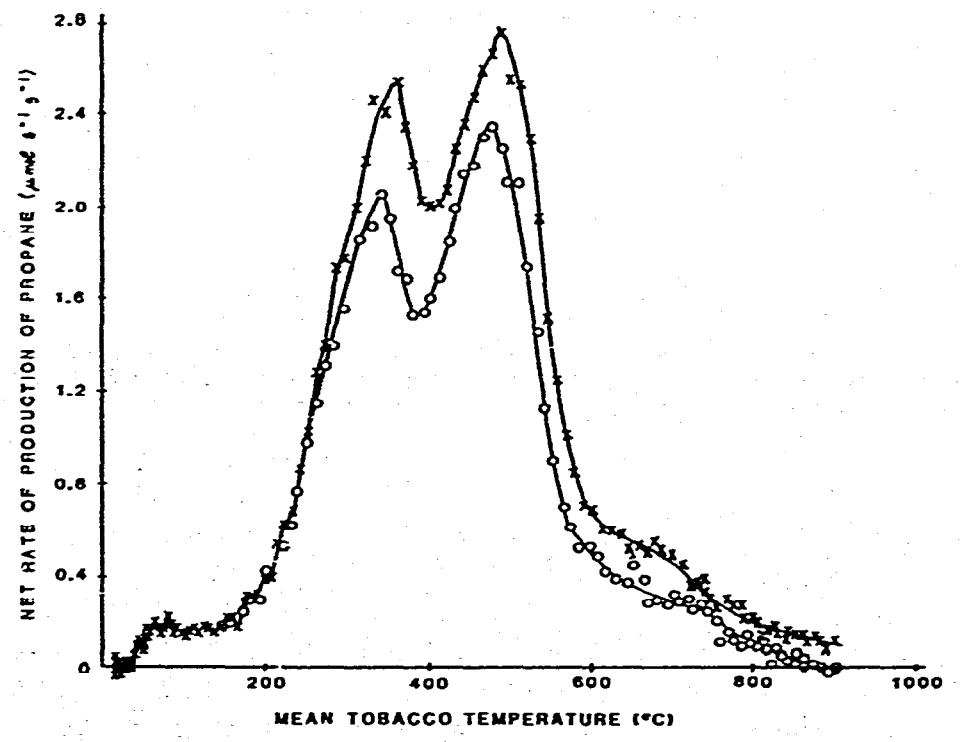

Fig. 1. Effect of varying the residence time of tobacco-pyrolysis products in the furnace on propane formation rates, under inert conditions. ×, Tobacco at furnace inlet; ⊙, tobacco at furnace outlet.

*In this Tabie, as in all tables of the present paper, the deconvolution of the profiles into low-temperature (20–400°C) and high-temperature (400–900°C) regions has been done by dividing the complete profile with vertical lines at 400 and 900°C. The deconvoluted figures in the tables are thus approximate only.

TABLE 1

EFFECT OF POSITION OF TOBACCO IN FURNACE ON TOTAL QUANTITIES OF GASES PRODUCED BY PYROLYSIS IN ARGON[a]

Position of tobacco in furnace	*Temp. range (°C)*	*Quantity of individual gases produced (μmol g⁻¹)*						
		H_2	CH_4	C_2H_6	C_3H_8	C_3H_6	CO	CO_2
Inlet	Low (20–400)			22	173		598	2,327
	High (400–900)			93	262		1,693	793
	Total (20–900)	2,552	665	115	435	44.0	2,291	3,120
Exit	Low (20–400)			21	139		518	2,095
	High (400–900)			82	235		1,392	803
	Total (20–900)	2,228	630	103	374	32.6	1,910	2,898

[a] 0.25 g of tobacco; inlet flow into furnace = 3.33 cm^3 sec^{-1}; mean tobacco heating rate = 1.9 K sec^{-1}.

TABLE 2

NET PROPORTION (%) OF PRODUCTS FORMED VIA HOMOGENEOUS REACTION OF INTERMEDIATE PRODUCTS

Temp. range (°C)	*Net proportion of products formed via homogeneous reaction of intermediates*[a]						
	H_2	CH_4	C_2H_6	C_3H_8	C_3H_6	CO	CO_2
Low (20–400)			2.3	10.9		7.2	5.2
High (400–900)			6.3	5.4		9.8	−0.6
Total (20–900)	6.8	2.7	5.5	7.5	15	9.1	3.7

[a] The quoted proportion refers to those products formed via intermediates when the reactant tobacco is at the average centre of the furnace. To a first approximation it is given by:

$$\text{Proportion} = \frac{Q_{\text{inlet}} - Q_{\text{exit}}}{2\bar{Q}} 100$$

where Q_{inlet} = quantity of gases produced with tobacco at inlet position (Table 1),
Q_{exit} = quantity of gases produced with tobacco at exit position (Table 1),
$\bar{Q}$ = mean of Q_{inlet} and Q_{exit}.

of volatile and semi-volatile intermediate products, the proportions of each being given in Table 2. Because of experimental error and the small quantities of hydrocarbons determined, the differences for the hydrocarbons may not be significant.

1.2 The effect of radical-chain propagation inhibitors

The effect of 1% v/v nitric oxide or nitrogen dioxide on the formation rate of carbon monoxide, for example, from tobacco pyrolysis is shown in Fig. 2. The total quantities of products formed are given in Table 3.

Hinshelwood[9] has stated that the most direct evidence for the participation of

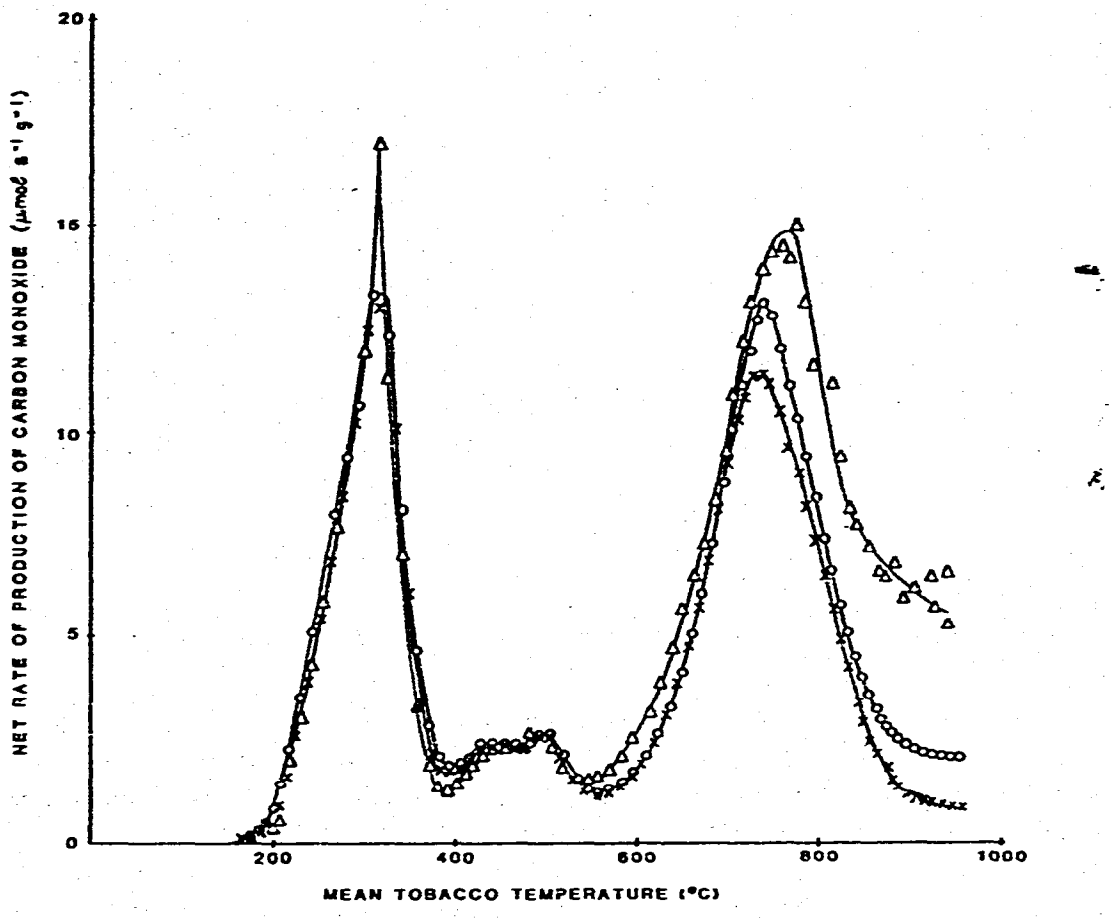

Fig. 2. Effect of nitrogen oxides on formation of carbon monoxide from tobacco decomposition. ×, Pyrolysed in 100% argon; ⊙, pyrolysed in 1% NO in argon; △, pyrolysed in 1% NO_2 in argon.

radical chain propagation steps in a reaction is obtained by studying the influence of nitric oxide, which preferentially reacts with chain centres in the system. Subsequently, most studies have assumed that nitric oxide suppresses the chain propagation steps, and that the net reaction occurring in the presence of nitric oxide is molecular. However, this assumption is not true: nitric oxide participates by setting up alternate chain reactions[10,11] and a measurable reaction rate can be obtained in the presence of nitric oxide even when there is no molecular contribution to the overall reaction[12]. Even though in certain hypothetical cases it can be shown that nitric oxide could have no overall effect on the rate of a chain reaction[10], it is a reasonable indication of the participation of radical chains if nitric oxide (or other radical additive) affects the formation rates of products.

The effect of the nitrogen oxides on the formation of hydrogen, methane, and propane (at least in the low-temperature region) is negligible. Propene apparently increases in the presence of nitric oxide, but this may not be significant in view of the large errors involved in measuring the small amounts of propene.

TABLE 3

EFFECT OF PYROLYSING TOBACCO IN THE PRESENCE OF NITROGEN OXIDES[a]

Pyrolysis atmosphere	*Temp. range (°C)*	*Quantity of individual gases produced (μmol g⁻¹)*						
		H_2	CH_4	C_2H_6	C_3H_8	C_3H_6	CO	CO_2
Ar	Low (20–400)			23.6	151		539	2,265
	High (400–950)			90.4	236		1,385	645
	Total (20–950)	2,290	597	114	387	36.2	1,924	2,910
Ar+1% v/v NO	Low (20–400)				142		569	2,593
	High (400–950)				271		1,701	807
	Total (20–950)	2,380	589	[b]	413	64.1	2,270	3,400
Ar+1% v/v NO_2	Low (20–400)				139		515	2,968
	High (400–950)				280		2,274	1,034
	Total (20–950)	2,378	626[c]	[b]	419	38.4	2,789	4,002

[a] 1.0 g of tobacco; inlet flow into furnace = 3.33 cm^3 sec^{-1}; mean tobacco heating rate = 2.1 K sec^{-1}.
[b] Excessive interference to $m/e = 30$ peak (used to monitor ethane) by nitric oxide and nitrogen dioxide. [c] Nitrogen dioxide also gives a peak at $m/e = 16$, which has not been corrected for.

The effect of both nitrogen oxides on carbon monoxide formation in the low-temperature region is small (<6%). In the presence of nitrogen dioxide, an abnormally high peak formation rate occurs at 320°C, although the total amount of carbon monoxide formed in the 20–400°C range is 4% lower than in the absence of nitrogen dioxide. The peak in carbon monoxide production at 320°C was probably due to heterogeneous decomposition of nitrogen dioxide into oxygen, and subsequent oxidation of the tobacco*.

The nitrogen oxides significantly increase the low-temperature formation of carbon dioxide, presumably by heterogeneous reaction with the reactant solid. Homogeneous reactions such as:

$$NO_2 + CO \rightarrow CO_2 + NO$$

are too slow in this temperature range to be significant**.

In the high-temperature region, both carbon oxide formation rates increase significantly in the presence of the nitrogen oxides. At these temperatures, the heterogeneous decomposition of nitrogen dioxide will have gone to completion, and oxidation of the solid reactant by oxygen and nitric oxide can occur.

Thus, although the effect of nitric oxide and nitrogen dioxide on tobacco pyrolysis is complex because of the resultant oxidation, there is no evidence for the

*Using the values of nitrogen dioxide concentration in the present system at 320°C, and rate constants calculated from published Arrhenius parameters[13], the homogeneous rate of decomposition of nitrogen dioxide is too slow to be significant in the present system at 320°C.
**For example, using published Arrhenius parameters[14] and the observed concentrations at 320°C, the calculated rate of this reaction is 1.3×10^{-5} μmol cm^{-3} sec^{-1}.

suppression of the formation of any of the gases monitored. Thus, it is probable that:

(a) the participation of radical chain reactions in the gas phase is negligible,
and (b) if radical chains are involved, they occur within the bulk solid, which must be inaccessible by mass transfer of the nitrogen oxides.

1.3 The effect of the inert gas and its space velocity

Virtually identical gas formation rate/temperature profiles were obtained when the tobacco was pyrolysed in helium, nitrogen and argon (flow of 3.33 cm^3 sec^{-1} into the reaction furnace). Furthermore, for the pyrolysis in argon, increasing the gas flow-rate into the furnace from 1.67 to 16.7 cm^3 sec^{-1} had only a small (secondary) effect on the profiles. Figure 3 illustrates the effect on the formation rate of ethane, for example, and Table 4 summarises the results for the total quantities of gases.

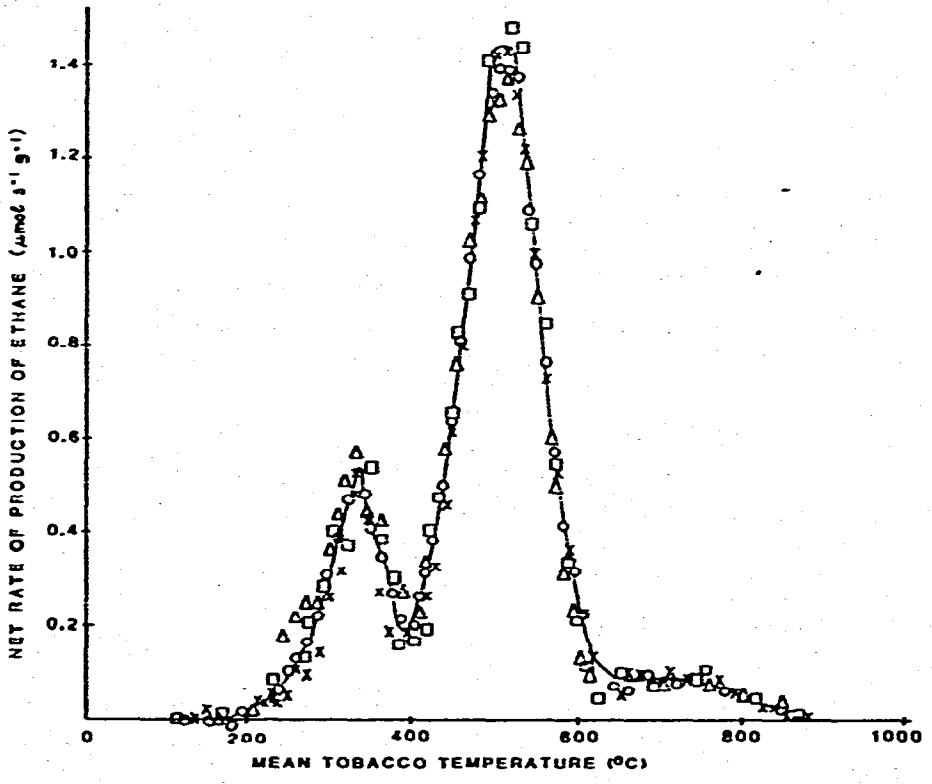

Fig. 3. Effect of inert gas flow-rate on production of ethane from tobacco pyrolysis in argon. Flow of argon into furnace (cm^3 sec^{-1}): ×, 1.67; ⊙, 3.33; ⊡, 8.33; △, 16.7.

Within the limits of the experimental error, the production of the hydrocarbon gases is effectively independent of flow-rate (the apparent effect given in Table 4, for ethane in the low-temperature region, for example, is seen to be within the scatter of data in Fig. 3). The total amount of hydrogen produced over the whole pyrolysis increases by 8% as the flow-rate is increased from 1.67 to 8.33 cm^3 sec^{-1}, and then

TABLE 4

EFFECT OF INERT GAS FLOW VELOCITY ON TOTAL GASES PRODUCED FROM PYROLYSIS OF TOBACCO*

Gas flow-rate into furnace ($cm^3\ sec^{-1}$)	*Temp. range* (°C)	*Quantity of individual gases produced* ($\mu mol\ g^{-1}$)						
		H_2	CH_4	C_2H_6	C_3H_8	C_3H_6	CO	CO_2
1.67	Low (20–400)			18.5	109		519	2,303
	High (400–950)			90.5	318		1,315	706
	Total (20–950)	2,191	616	109	427	48.2	1,834	3,009
3.33	Low (20–400)			23.6	151		539	2,265
	High (400–950)			90.4	236		1,385	645
	Total (20–950)	2,290	597	114	387	36.2	1,924	2,910
8.33	Low (20–400)			23.1	174		567	2,415
	High (400–950)			79.3	277		1,423	640
	Total (20–950)	2,370	620	102.4	451	36.0	1,990	3,055
16.67	Low (20–400)			31.0	164		596	2,226
	High (400–950)			77.6	204		1,436	606
	Total (20–950)	2,367	611	108.6	368	36.5	2,032	2,832

* 1.0 g of tobacco, pyrolysed in argon at 2.1 K sec^{-1}.

remains constant. The carbon dioxide profile is unaffected by flow up to about 550°C although the total high-temperature carbon dioxide produced decreases with increasing flow (Table 4). The carbon monoxide profiles increase slightly but systematically with flow-rate.

However, all the above trends are very much second order effects—varying the flow-rate over a ten-fold range affects most of the gas production rates by less than 10%. From a detailed examination of this observation in Section 1.8 of the Discussion, it is concluded that the decomposition of tobacco is controlled by the kinetics of the chemical reactions involved and not by the physical processes of diffusion of the product gases within the bulk gas phase.

1.4 The effect of carbon dioxide on tobacco pyrolysis

The effect of pyrolysing tobacco in the presence of 11% v/v carbon dioxide/89% v/v nitrogen on the production of the carbon oxides is shown in Fig. 4. These profiles are identical up to about 550°C to those obtained under identical conditions in nitrogen. Above this temperature, the net carbon dioxide rate of production falls below that in pure nitrogen; above 600°C it falls below the input rate. At the same time the rate of production of carbon monoxide rises above that in pure nitrogen.

At temperatures above about 550°C, the endothermic heterogeneous reduction of carbon dioxide by the carbonaceous reactant becomes progressively more important.

In Fig. 4 it is seen that when tobacco is pyrolysed in nitrogen, there is a small net

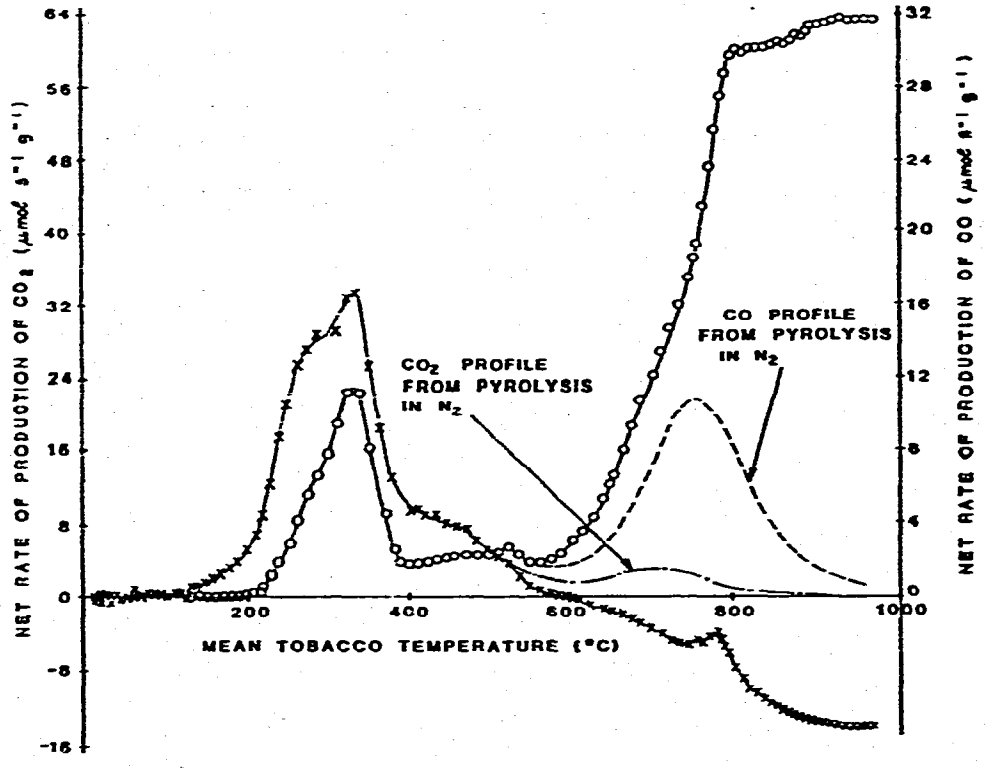

Fig. 4. Effect of pyrolysing tobacco in 11% v/v carbon dioxide–89% v/v nitrogen. Tobacco heated at 2.1 K sec^{-1}; input CO_2 flow = 14.8 μmol sec^{-1}. ×, CO_2 (left-hand axis); ⊙, CO (right-hand axis).

production of carbon dioxide above 550°C, even though this concentration is readily consumed when the tobacco is pyrolysed in 11% carbon dioxide. The rate of reduction of carbon dioxide is proportional to its concentration in the gas phase. Thus, during the pyrolysis of tobacco, the low carbon dioxide concentration produced above 550°C means that only a small proportion of the total carbon monoxide produced in the high-temperature region is formed via carbon dioxide.

The effect of varying the flow-rate of the carbon dioxide/nitrogen gas mixture is shown in Figs. 5 and 6 for carbon dioxide and the product carbon monoxide, respectively. The flow-rate has no effect until the reduction of carbon dioxide starts to become effective at temperatures above about 500°C. Above this temperature, the rate of production of carbon monoxide, and the rate of consumption of carbon dioxide, both increase with increasing flow-rate. It is shown in Section 1.6 that this increase in rate is caused by kinetic effects rather than the overall reaction being controlled by mass transfer processes. Since the exit carbon dioxide flow-rate differs appreciably from the inlet, an increase in gas flow-rate increases the intrinsic rate of reaction by increasing the average carbon dioxide concentration within the reaction zone. However, at temperatures above 850°C when the inlet flow to the furnace is 1.67 cm^3 sec^{-1}, all the carbon dioxide is consumed (Fig. 5). Under these conditions, the mass

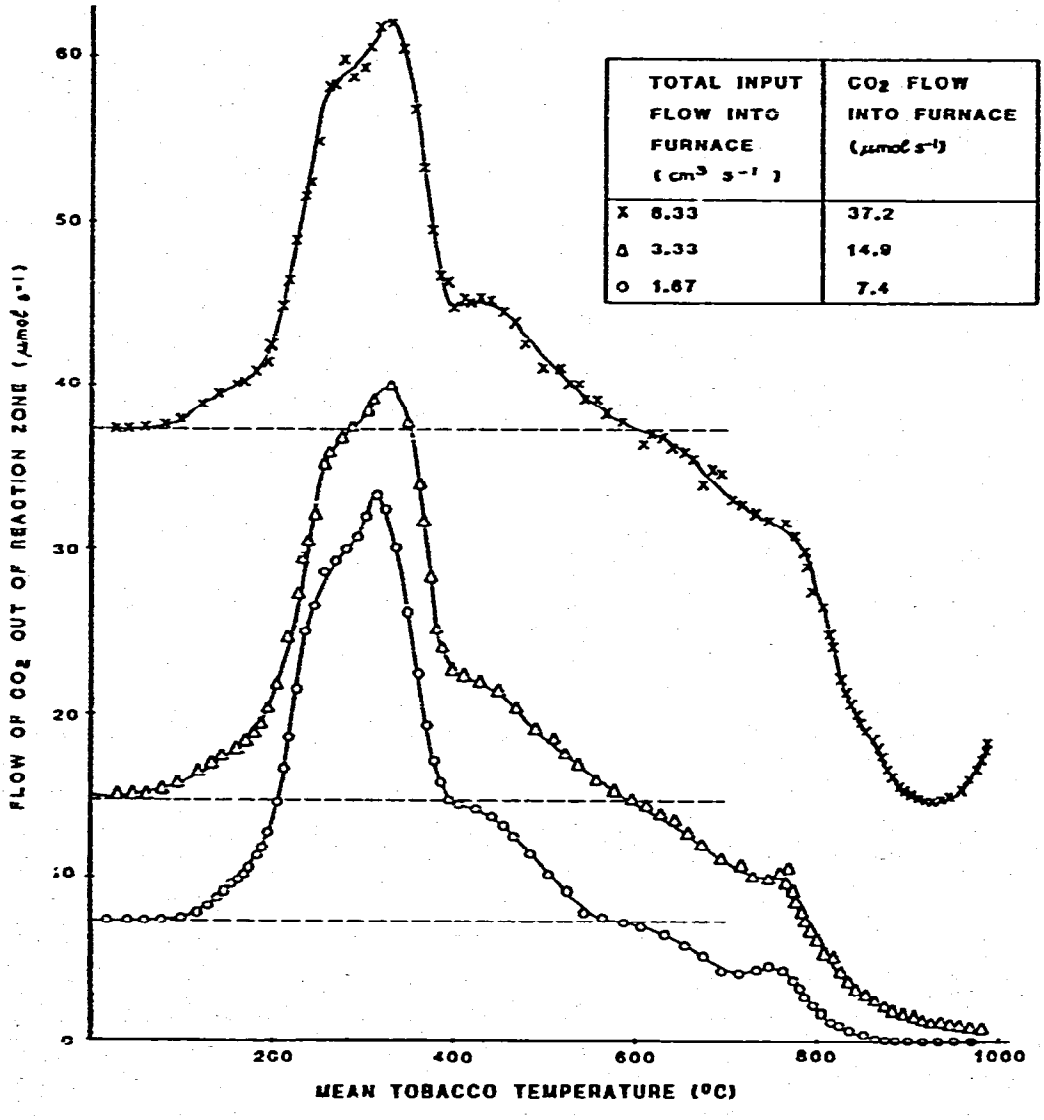

Fig. 5. Effect of gas flow-rate into furnace on resultant flow of carbon dioxide, when tobacco is pyrolysed in 11% v/v carbon dioxide–89% v/v nitrogen. Tobacco heated at 1.7 K sec^{-1}.

trasfer of carbon dioxide into the reaction zone is also effective in controlling the reaction rate.

1.5 The effect of carbon monoxide on tobacco pyrolysis

Figure 7 indicates that below 550°C pyrolysis of tobacco in the presence of 9.7% v/v carbon monoxide inhibits the formation of both oxides of carbon, whereas above 550°C the formation of carbon monoxide is decreased while that of carbon dioxide is increased. The mechanistic interpretation of these results is discussed in Section 1.7.

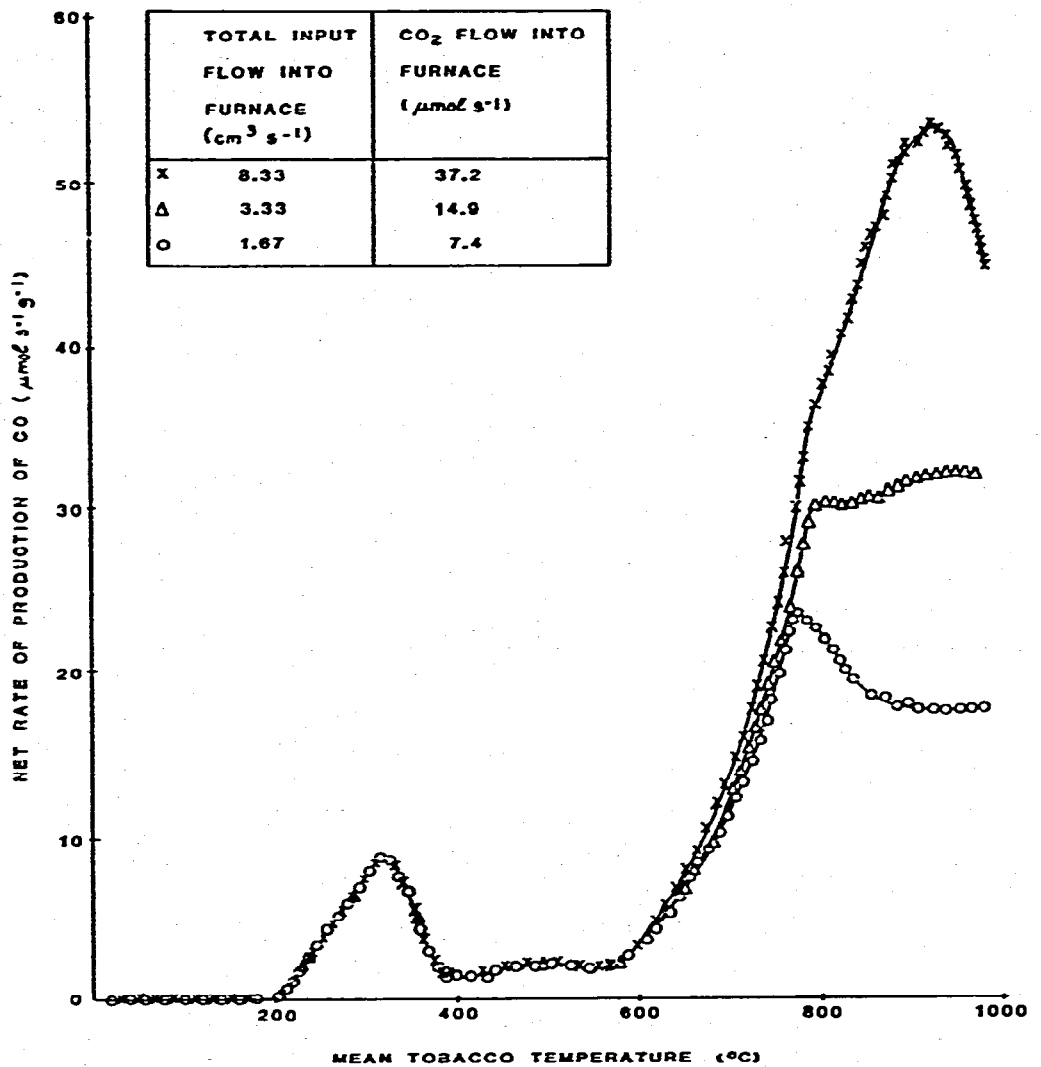

Fig. 6. Effect of gas flow-rate into furnace on production of carbon monoxide from pyrolysis of tobacco in 11% v/v carbon dioxide–89% v/v nitrogen. Tobacco heated at 1.7 K sec^{-1}.

Discussion

There are five main stages to the reaction between a gas and a porous solid:

1. Mass transport of the reactant gas from the bulk gas phase to the solid surface by diffusion and convection.
2. Diffusion of the reactant gas into the pores of the solid.
3. Chemical reaction of the gas and solid, which can include adsorption of reactant molecules, and desorption of product molecules, from both the outer and inner surfaces of the solid.
4. Diffusion of product gases out of the pores of the solid.
5. Removal of product gases away from the surface, into the bulk phase.

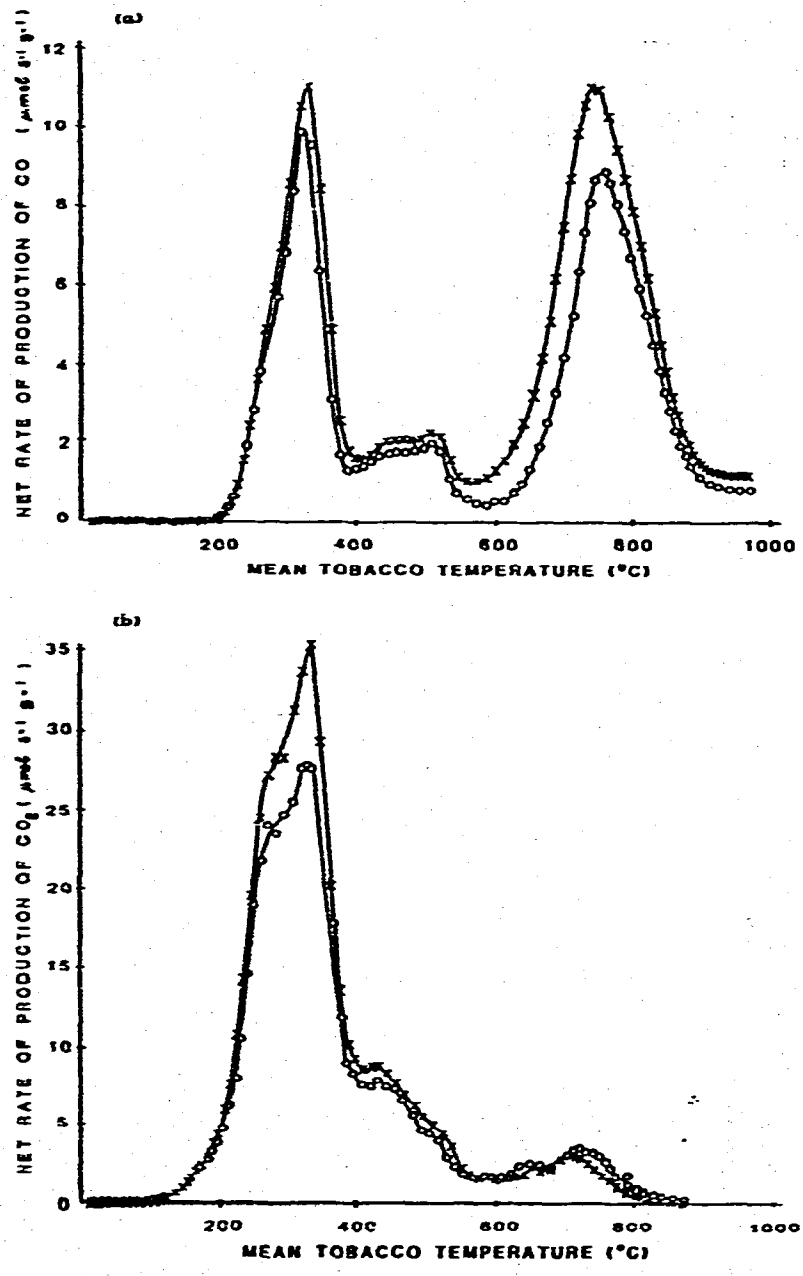

Fig. 7. Effect of pyrolysing tobacco in 9.7% v/v carbon monoxide–90.3% v/v nitrogen on the formation of (a) carbon monoxide and (b) carbon dioxide. ×, Pyrolysed in 100% N_2; ⊙, pyrolysed in 9.7% CO–90.3% N_2.

In practice, it is often found that within a given temperature regime, one of the three major processes (bulk phase diffusion, internal pore diffusion, or chemical reaction) is much slower than the other two[15,16]. Consequently the overall reaction rate is limited by the rate of this process. In the analytical treatment of the present study, only two processes are considered: bulk diffusion and chemical kinetics. The

effect, if any, of diffusion within single tobacco stands could be more profitably examined by computer modelling of the system.

1.6 The reaction of tobacco with carbon dioxide

The generalised reaction sequence is:

1. $S \rightarrow (CO)_s$
2. $S \rightarrow (CO_2)_s$
3. $S+(CO_2)_s \rightarrow n(CO)_s$
4. $(CO)_s \rightleftharpoons (CO)_g$
5. $(CO_2)_s \rightleftharpoons (CO_2)_g$

where S represents reactant solid (tobacco),
subscripts s and g refer to the gases adjacent to the reactant surface and in the bulk gas phase, respectively,
n is a stoichiometric factor,
and reaction steps 4 and 5 represent diffusion across the boundary layer.

The net rate of accumulation of carbon monoxide in the gas phase, $d(CO)_g/dt$ (μmol sec^{-1} g^{-1}, i.e., per g of tobacco), due to diffusion across the boundary layer, is given by Fick's Law:

$$\frac{d(CO)_g}{dt} = -D_{CO} A \frac{d[CO]}{dx} = b_4([CO]_s - [CO]_g) \quad (1)$$

where D_{CO} is the diffusion coefficient of carbon monoxide (cm^2 sec^{-1}),
A is the surface area per g of tobacco strands (cm^2 g^{-1}),
$d[CO]/dx$ is the concentration gradient of carbon monoxide across the boundary layer (μmol cm^{-4}),
[CO] is the concentration of carbon monoxide (μmol cm^{-3}),
and b_4 is the mass transport coefficient of carbon monoxide through the boundary layer (cm^3 sec^{-1} g^{-1}, i.e., per g of tobacco) given by:

$$b_4 = -\frac{D_{CO} A}{\delta} = -\frac{D_{CO} A(Nu)}{L} \quad (2)$$

where δ is the thickness of the boundary layer (cm).

The value of δ is equal to $L/(Nu)$, where L is a characteristic length dimension (cm), e.g., strand thickness, and (Nu) is the Nusselt number[17].

Similarly, for carbon dioxide:

$$\frac{d(CO_2)_g}{dt} = b_5([CO_2]_s - [CO_2]_g) \quad (3)$$

The values of $[CO]_s$ and $[CO_2]_s$ adjacent to the surface depend on the kinetic mechanism of the reaction at the surface. Under stationary or quasi-stationary conditions, the kinetic rate is equal to the rate at which the reactant reaches the

surface by diffusion. The unknown surface concentrations in eqns (1) and (3) can be eliminated to give the following equations for the rates of formation of products:

$$\frac{d(CO)_g}{dt} = k_1[S] + \frac{nk_3[S]}{k_3[S]+b_5}(k_2[S]+b_5[CO_2]_g) \tag{4}$$

$$\frac{\Delta d(CO_2)_g}{dt} = \frac{b_5[S]}{k_3[S]+b_5}(k_2-k_3[CO_2]_g) \tag{5}$$

where $\Delta d(CO_2)_g/dt$ is the net production rate of carbon dioxide (μmol sec^{-1} g^{-1})*, equal to the total rate of carbon dioxide flowing out of the reaction zone less the carbon dioxide flow in,

and k_j is the rate constant of the reaction numbered "j".

The mean bulk concentration of carbon dioxide in the reaction zone, $[CO_2]_g$ (μmol cm^{-3}) is given by:

$$[CO_2]_g = \frac{1}{F}\cdot\overline{\frac{d(CO_2)_g}{dt}} \tag{6}$$

where $\overline{d(CO_2)_g/dt}$ is the average micromolar flow of carbon dioxide inside the reaction zone (μmol sec^{-1}), equal to the mean of the micromolar flow of carbon dioxide into and out of the reaction zone,

and F is the mean total volumetric gas flow in the reaction zone (cm^3 sec^{-1}), given by:

$$F = \frac{F_{in}+F_{out}}{2}\cdot\frac{T}{T_0} \tag{7}$$

where F_{in} and F_{out} are the gas flows into and out of the reaction zone,

T is the temperature (K) of the reaction zone,

and T_0 is the ambient temperature at which F_{in} and F_{out} were measured.

Furthermore, various experimental and theoretical studies[16] have shown that the mass transfer coefficient is proportional to the square root of the gas flow, i.e.

$$b_4 = h_4\sqrt{F} \tag{8}$$

where h_4 is a constant of proportionality.

Thus substituting eqns (6) and (8) into eqn (4), and the equivalent equations for carbon dioxide into eqn (5), gives:

$$\frac{d(CO)_g}{dt} = k_1[S] + \frac{nk_3[S]}{k_3[S]+h_5\sqrt{F}}\left\{k_2[S] + \frac{h_5}{\sqrt{F}}\cdot\overline{\frac{d(CO_2)_g}{dt}}\right\} \tag{9}$$

$$\frac{\Delta d(CO_2)_g}{dt} = \frac{h_5\sqrt{F}[S]}{k_3[S]+h_5\sqrt{F}}\left\{k_2 - \frac{k_3}{F}\overline{\frac{d(CO_2)_g}{dt}}\right\} \tag{10}$$

*$\Delta d(CO_2)_g/dt$ will be numerically negative if there is a net consumption of carbon dioxide.

The observed variation of the carbon oxides net reaction rates with gas flow (Figs. 5 and 6) can now be compared to the variation predicted by eqns (9) and (10), for kinetic control and diffusion control of the reaction.

Kinetic control. Under kinetic control conditions, $h_5\sqrt{F} \gg k_3[S]$ and $h_5\overline{(d(CO_2)_g/dt)}/\sqrt{F} \gg k_2[S]$. Equations 9 and 10 reduce to:

$$\frac{d(CO)_g}{dt} = k_1[S] + nk_3[S] \cdot \frac{\overline{d(CO_2)_g}}{dt} \cdot \frac{1}{F} \tag{11}$$

$$\frac{\Delta d(CO_2)_g}{dt} = k_2[S] - k_3[S] \cdot \frac{\overline{d(CO_2)_g}}{dt} \cdot \frac{1}{F} \tag{12}$$

The mass transfer coefficients do not appear in eqns (11) and (12), and the reaction rates are controlled entirely by the kinetics of the reaction. Thus, if [S] is relatively large, so that to a first approximation it is independent of tobacco consumed*, then eqn (11) predicts that a plot of $d(CO)_g/dt$ against $\overline{(d(CO_2)_g/dt)}/F$ is linear with a positive gradient, and eqn (12) predicts that a plot of $\Delta d(CO_2)_g/dt$ against $\overline{(d(CO_2)_g/dt)}/F$ is linear with a negative gradient. In fact, the above assumption regarding [S] is not true above about 900°C for the largest flow-rates used, since the minimum at 930°C in the plot in Fig. 5 for a furnace inlet flow of 8.33 $cm^3\ sec^{-1}$ indicates that all the tobacco has been consumed. However, the assumption below 900°C should be valid, and the rate parameters are plotted according to eqns (11) and (12) in Fig. 8, at temperatures between 600 and 900°C, the values being interpolated from the data in Figs. 5 and 6.

The plots in Fig. 8 are exactly as predicted by eqns (11) and (12), except that at temperatures above 850°C, the reaction rates ($d(CO)_g/dt$ and $\Delta d(CO_2)_g/dt$) at the lowest flow-rates fall below the linear extrapolation of the higher flows This occurs because the input carbon dioxide flow is completely consumed at 860°C at the lowest total flow-rate (Fig. 5), and so under these conditions the reaction is controlled by the mass transfer of carbon dioxide into the reaction zone. However, under the majority of experimental conditions used, the plots in Fig. 8 are in accordance with eqns (11) and (12), indicating that the reaction is controlled by kinetic effects.

Values of $k_3[S]$ and n obtained from the gradients of the plots in Fig. 8 are given in Table 5. Above 700°C the value of n is 2.1 ± 0.3, which is the stoichiometric value in the reduction by carbon:

$$C + CO_2 \rightarrow 2CO$$

The values of $k_3[S]$ in Table 5 are not those which would be obtained when tobacco is pyrolysed in an inert atmosphere, because above about 600°C in an 11% carbon dioxide atmosphere the reaction rate and hence the value of [S] is dominated by the reduction of carbon dioxide (Fig. 4). This reduction only occurs to a relatively small extent in an inert atmosphere, resulting in a different value for [S] and hence $k_3[S]$.

*This assumption is justified in Section 2.4.

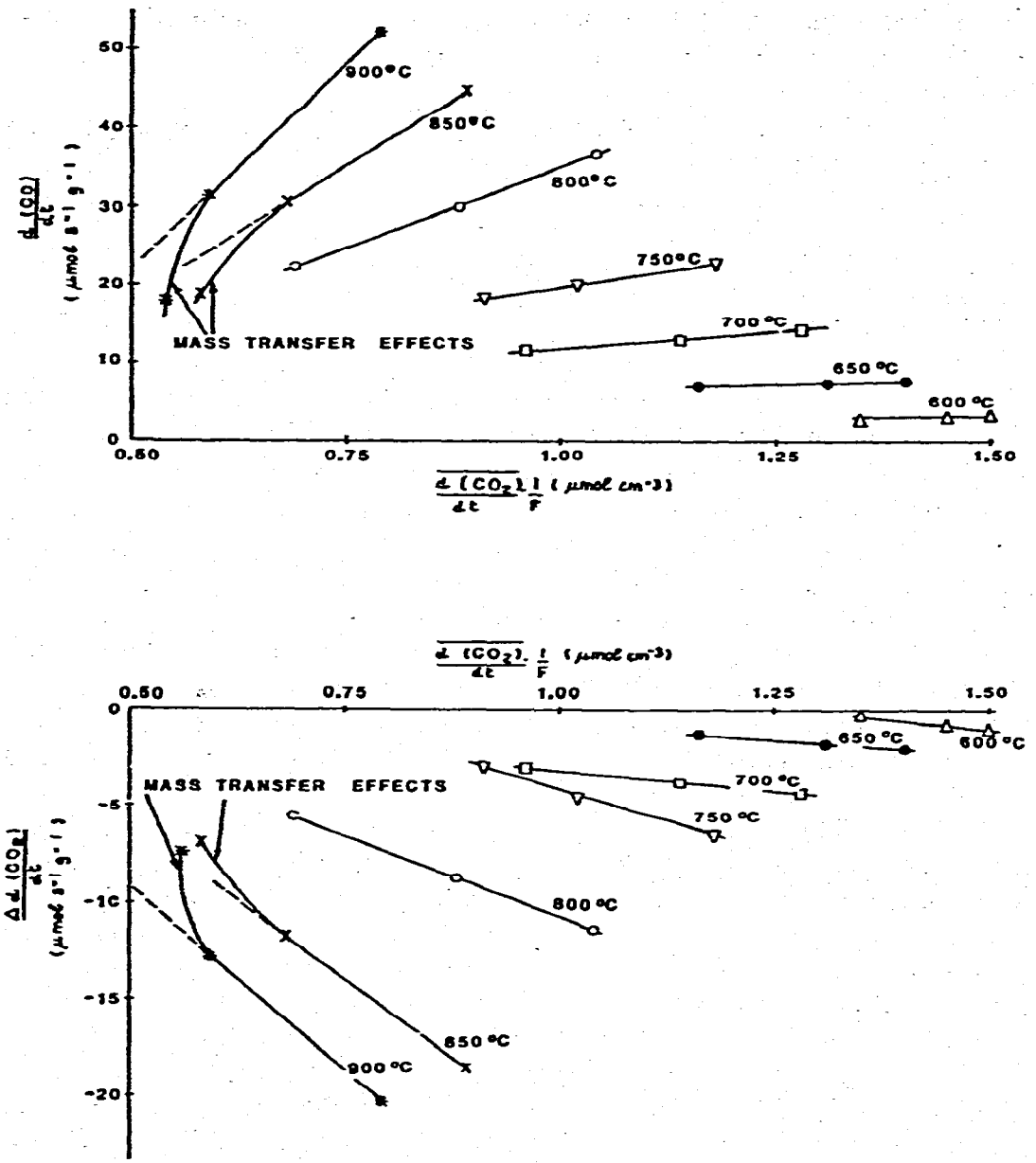

Fig. 8. Tobacco/carbon dioxide reaction: reaction rates plotted using kinetic-control equation.

Diffusion control. Under diffusion control conditions, $h_5\sqrt{F} \ll k_3[S]$ and $h_5\overline{(d(CO_2)_g/dt)}/\sqrt{F} \ll k_2[S]$. Thus eqns (9) and (10) reduce to:

$$\frac{d(CO)_g}{dt} = k_1[S] + nk_2[S] \tag{13}$$

$$\frac{\Delta d(CO_2)_g}{dt} \cdot \frac{1}{\sqrt{F}} = \frac{h_5 k_2}{k_3} - h_5 \cdot \overline{\frac{d(CO_2)_g}{dt}} \cdot \frac{1}{F} \tag{14}$$

TABLE 5

RATE CONSTANT VALUES FOR THE OVERALL REDUCTION OF CARBON DIOXIDE BY TOBACCO*

Temp. (°C)	nk_3[S] ($cm^3\ sec^{-1}\ g^{-1}$)	k_3[S] ($cm^3\ sec^{-1}\ g^{-1}$)	n
600	1.39	4.87	0.29
650	3.27	3.20	1.02
700	8.60	5.06	1.70
750	17.3	9.90	1.75
800	40.0	16.4	2.44
850	67.0	32.0	2.09
900	102	45.0	2.27

* $S + CO_2 \rightarrow nCO$, where S is tobacco substrate and n is a stoichiometric factor.

Equation (13) predicts that $d(CO)_g/dt$ is dependent only on the rate constants, i.e., temperature. Equation 14 predicts that a plot of $(\Delta d(CO_2)_g/dt)/\sqrt{F}$ against $\overline{(d(CO_2)/dt)}/F$ is linear with a negative gradient. Since Fig. 8 shows that $d(CO)_g/dt$ is linearly related to $\overline{(d(CO_2)_g/dt)}/F$, the prediction of eqn (13) is incorrect. Furthermore, when the results are plotted according to eqn (14), the plots are distinctly non-linear. Consequently, the predictions of both diffusion control equations are incorrect, confirming that the reaction is controlled kinetically.

The above mechanism is, however, simplified, since it does not take into account the inhibition of the carbon dioxide reduction by carbon monoxide. There have been many studies reported in the literature on the reaction between carbon* or coal and carbon dioxide and the empirical characteristics of the reaction kinetics are well defined[16,18]. Although the exact mechanism is probably dependent on the nature of the carbon surface, the postulated mechanism for which there is the most evidence[16,18–21] consists of the following reaction steps:

6. $C + CO_2 \rightleftharpoons C(O)_{ads} + CO$
7. $C(O)_{ads} \rightarrow CO$

where $C(O)_{ads}$ represents an adsorbed oxygen atom on the carbonaceous surface.

The effect of carbon monoxide on tobacco pyrolysis is discussed in the next section.

1.7 The reaction of tobacco with carbon monoxide

Since the simplified tobacco/carbon dioxide mechanism has been shown to be kinetically controlled and the effect of carbon monoxide is effectively an inhibition of that reaction, only kinetic control is considered in this section.

High-temperature region. A mechanism for the effect of carbon monoxide, consistent with reactions 6 and 7 above is:

*The carbons have generally been ill-defined and possibly contain trace impurities.

1. $S \rightarrow CO$
2. $S \rightarrow CO_2$
8. $S \rightarrow C(O)_{ads}$
6. $C + CO_2 \rightleftharpoons C(O)_{ads} + CO$
7. $C(O)_{ads} \rightarrow CO$

The amount of carbon dioxide produced in the high-temperature region is small, so that the rate of the forward reaction 6 is considered to be kinetically insignificant. Consequently, the net rate of formation of carbon monoxide is given by:

$$\frac{\Delta d(CO)}{dt} = k_1[S] - k_{-6}[CO]\theta_0 + k_7\theta_0 \tag{15}$$

where $\Delta d(CO)/dt$ is equal to the total rate of carbon monoxide flowing out of the reaction zone, less the carbon monoxide flow in

and θ_0 is the fraction of the free sites on the carbonaceous solid covered with adsorbed oxygen atoms.

The steady state condition for adsorbed oxygen atoms is given by:

$$k_8[S] = k_{-6}[CO]\theta_0 + k_7\theta_0 \tag{16}$$

Thus substituting the value of θ_0 from eqn (16) into eqn (15) gives:

$$\frac{\Delta d(CO)}{dt} = k_1[S] + k_8[S]\left\{\frac{k_7 - k_{-6}[CO]}{k_7 + k_{-6}[CO]}\right\} \tag{17}$$

Similarly, the rate of formation of carbon dioxide is given by:

$$\frac{d(CO_2)}{dt} = k_2[S] + \frac{k_8[S]}{1 + \frac{k_7}{k_{-6}}\frac{1}{[CO]}} \tag{18}$$

Thus, eqns (17) and (18) predict that increasing the value of [CO] will decrease the value of $\Delta d(CO)/dt$ and increase the value of $d(CO_2)/dt$. This prediction is observed to occur in practice at temperatures above about 550°C (Fig. 7), thus supporting the postulated mechanism.

Low-temperature region. In the low-temperature region, the presence of carbon monoxide depresses the formation of carbon monoxide to a small extent, and that of carbon dioxide to a larger extent (Fig. 7). This trend indicates that at least a proportion of the carbon dioxide is formed from an "activated" form of the reactant tobacco, and that carbon monoxide can react with the "activated" form to give a product other than carbon dioxide.

1. $S \rightarrow CO$
2a. $S \rightarrow CO_2$
2b. $S \rightarrow S^*$

2c. $S^* \rightarrow CO_2$

9. $S^* + CO \rightarrow$ product

Reaction 9 could be an adsorption process.

Thus, for a stationary concentration of the "activated" reactant S^*, the reaction rates are given by eqns (19) and (20), which predict the observed effects of varying [CO].

$$\frac{\Delta d(CO)}{dt} = k_1[S] - \frac{k_{2b}[S]}{1 + \frac{k_{2c}}{k_9}\frac{1}{[CO]}} \tag{19}$$

$$\frac{d(CO_2)}{dt} = k_{2a}[S] + \frac{k_{2b}k_{2c}[S]}{k_{2c} + k_9[CO]} \tag{20}$$

1.8 Mechanism for the pyrolysis of tobacco in an inert atmosphere

A kinetic-controlled mechanism is considered first of all.

Low-temperature region. Using the mechanism developed in Section 1.7, and including the decomposition of intermediates, the complete generalised mechanism in the low-temperature region consists of reactions 1, 2a, 2b, 2c, and 9–14.

10. $S \rightarrow I$

11. $I \rightarrow mCO$

12. $I \rightarrow qCO_2$

13. $I \rightarrow$ other product

14. $I \rightarrow$ removed from reaction zone by flow of inert gas

where I represents all the volatile or semi-volatile intermediates which can decompose homogeneously into carbon monoxide or carbon dioxide,

and m and q are stoichiometric factors.

If the intermediates I and "activated" reactant S^* are present in stationary concentrations, the rates of formation of the carbon oxides are given by eqns (21) and (22).

$$\frac{d(CO)}{dt} = k_1[S] - \underbrace{\frac{k_{2b}[S]}{1 + \frac{k_{2c}F}{k_9\overline{d(CO)/dt}}}}_{A} + \underbrace{\frac{mk_{10}k_{11}[S]}{k_{11}+k_{12}+k_{13}+F/M}}_{B} \tag{21}$$

$$\frac{d(CO_2)}{dt} = k_{2a}[S] + \underbrace{\frac{k_{2b}k_{2c}[S]}{k_{2c} + \frac{k_9}{F}\cdot\overline{\frac{d(CO)}{dt}}}}_{C} + \underbrace{\frac{qk_{10}k_{12}[S]}{k_{11}+k_{12}+k_{13}+F/M}}_{D} \tag{22}$$

where F is the mean total volumetric gas flow in the reaction zone ($cm^3\ sec^{-1}$), given by eqn (7) above,
M is the mass of tobacco in the reaction zone (g),
and the rate of the mass transport reaction step 14 is equal to $[I]F/M$.

Since it is observed that variation of gas flow has only a secondary effect on $d(CO)/dt$, at a given temperature the only significant variable on the right-hand side of eqns (21) and (22) is F. As F increases, the values of A and B on the right-hand side of eqn (21) decrease. It is observed (Table 4) that carbon monoxide in the low-temperature region increases slightly with flow. Thus the value of A, which is negative in eqn (21), is more sensitive to the value of F than B.

As F increases, the value of C in eqn (22) increases, while that of D decreases. Since carbon dioxide formed in the low-temperature region is insensitive to flow (Table 4), then the magnitudes of C and D must be approximately equal.

High-temperature region. Using the mechanism developed in Section 1.7, and including the decomposition of intermediates, the complete generalised mechanism in the high-temperature region consists of reactions 1, 2, 6, 7, 8 and 10–14. As in Section 1.7, the rate of the forward reaction 6 is considered to be kinetically insignificant because of the relatively small amounts of carbon dioxide produced in the high-temperature region. Thus, assuming stationary concentrations for the intermediates I, the formation rates of the carbon oxides are given by:

$$\frac{d(CO)}{dt} = k_1[S] + \underbrace{k_8[S]\left\{\frac{k_7 - k_{-6}\overline{(d(CO)/dt)/F}}{k_7 + k_{-6}\overline{(d(CO)/dt)/F}}\right\}}_{E} + \underbrace{\frac{mk_{10}k_{11}[S]}{k_{11}+k_{12}+k_{13}+F/M}}_{G} \tag{23}$$

$$\frac{d(CO_2)}{dt} = k_2[S] + \underbrace{\frac{k_8[S]}{1+\dfrac{k_7F}{k_{-6}\overline{(d(CO)/dt)}}}}_{H} + \underbrace{\frac{qk_{10}k_{12}[S]}{k_{11}+k_{12}+k_{13}+F/M}}_{J} \tag{24}$$

On the right-hand side of eqn (23), the value of the combined term E increases as F increases, while the value of G decreases as F increases. Consequently, the observed small increase in carbon monoxide with flow in the high-temperature region (Table 4) is due to E being more sensitive to flow than G.

In eqn (24), the values of both H and J decrease with increasing F. Hence $d(CO_2)/dt$ systematically decrases with increasing flow in the high-temperature region (Table 4).

Consequently, the observed effects of space velocity on the formation of the carbon oxides from tobacco decomposition over the complete temperature range studied can be completely accounted for by a general kinetically controlled mechanism. The mechanism is entirely consistent with the independently observed effects of

conducting the pyrolysis in the presence of excess of either carbon dioxide or carbon monoxide. It is, therefore, concluded that bulk phase diffusion plays no part in the formation mechanism of gases by the pyrolysis of tobacco in an inert atmosphere. This conclusion is further substantiated by the absence of any observed effect on the gas formation rate temperature profiles when the tobacco is pyrolysed in helium, nitrogen, or argon.

Further support for this conclusion is obtained by considering the predicted implications of a diffusion-controlled mechanism. For the decomposition of tobacco in an inert atmosphere, there is no reactant gas to diffuse to the surface, and so only processes 3, 4 and 5 are possible (see first paragraph of Discussion). Under diffusion-controlled conditions, the diffusion of products away from the surface is rate-limiting. The further reaction of the products carbon monoxide and carbon dioxide is relatively small, and will take place before they have diffused from the surface. Product concentrations corresponding to the saturation concentrations are established at the surface. The rate of accumulation of carbon monoxide in the bulk gas phase, for example, is given by:

$$\frac{d(CO)_g}{dt} = b_4([CO]_{ss} - [CO]_g) = b_4[CO]_{ss} = h_4\sqrt{F}[CO]_{ss} \qquad (25)$$

since $[CO]_{ss} \gg [CO]_g$ under diffusion control, where $[CO]_{ss}$ is the saturated surface concentration of carbon monoxide, which is a function of temperature only.

Thus, at a given temperature, eqn (25) predicts that the rate of a diffusion-controlled reaction is directly proportional to $\sqrt{F}$. This is not so at any temperature, confirming that the reaction is not diffusion-controlled.

An alternate type of mechanism to those discussed above is that *all* the carbon oxides formed from tobacco are secondary products which largely decompose homogeneously in the vicinity of the reactant surface. However, the predicted kinetic expressions from permutations of this type of mechanism have a flow dependence on the reaction rates which is not observed.

PART 2. FACTORS AFFECTING THE PYROLYSIS OF TOBACCO IN AN ATMOSPHERE CONTAINING OXYGEN

Results

2.1 The effect of oxygen concentration in the pyrolysis atmosphere

In this Section, the results obtained when tobacco was pyrolysed in an atmosphere containing 0%, 9% and 21% v/v oxygen in nitrogen are compared. The inlet flow of gas to the furnace was 3.33 $cm^3\ sec^{-1}$ in all cases. The mean heating rates were 1.9, 2.1 and 2.6 $K\ sec^{-1}$, respectively, at each oxygen concentration, due to the exothermicity of the combustion.

The consumption of oxygen as a function of temperature is illustrated in Fig. 9. A measurable consumption of oxygen occurs at temperatures as low as 200°C. When

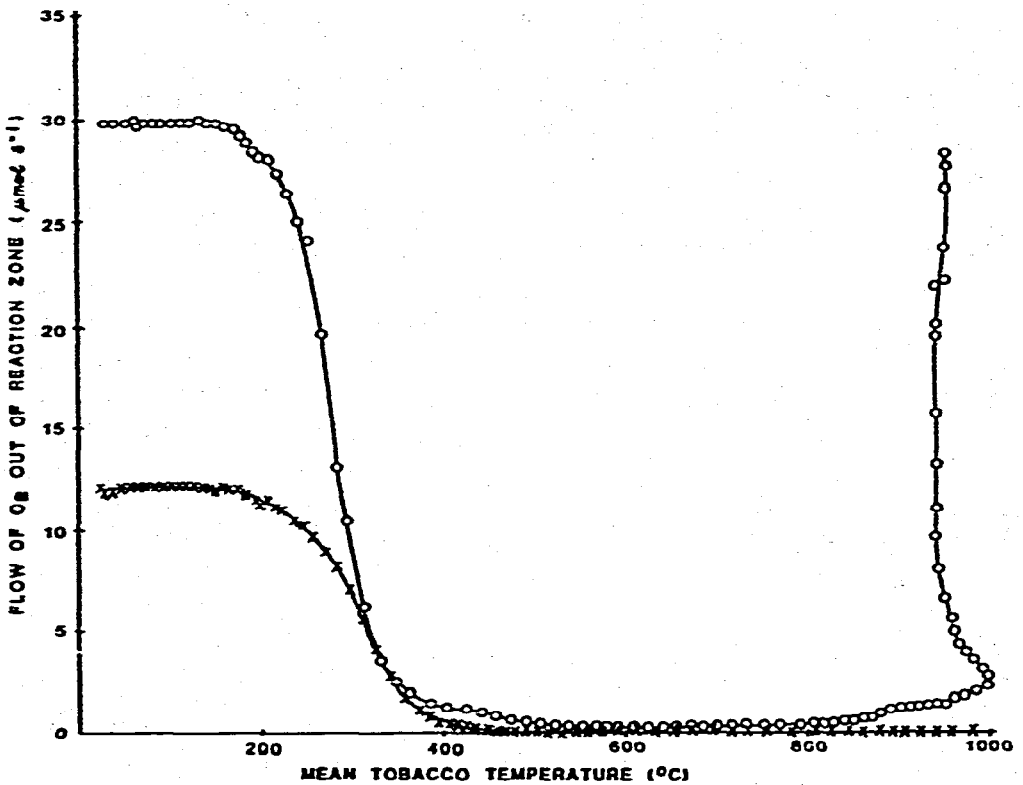

Fig. 9. Effect of oxygen concentration on the consumption of oxygen by tobacco combustion. ×, Initial $[O_2] = 9\%$ v/v in nitrogen; ⊙, initial $[O_2] = 21\%$ v/v in nitrogen.

the pyrolysis atmosphere initially contains 9% v/v oxygen, the oxygen is completely consumed at 460°C. However, when the initial oxygen concentration is 21% v/v, it is never completely consumed, and reaches a minimum mass flow of 0.3–0.4 μmol sec^{-1} over the temperature range 500 to 840°C. Above this temperature, the oxygen flow increases due to the consumption of tobacco. The negative gradient of the plot between 950 and 1000°C is due to the subsiding of the exothermic combustion reactions, as discussed previously[6].

The effect that the oxygen concentration in the pyrolysis atmosphere has on the formation of methane, for example, is shown in Fig. 10. The total amounts of products formed up to 950°C are given in Table 6.

The rates of formation of both oxides of carbon are extremely sensitive to oxygen concentration, especially above about 400°C, where the combustion reactions are dominant. The observed trends have been discussed previously[6].

Increasing the oxygen concentration decreases the total quantity of both hydrogen and methane formed, but extends the temperature range over which they are produced (Fig. 10). The hydrogen concentration is not reduced to zero in the presence of oxygen, because the explosion limits will be inhibited by the small amounts of hydrocarbons present[22]. The effect on propane and propene production is more complex (Table 6).

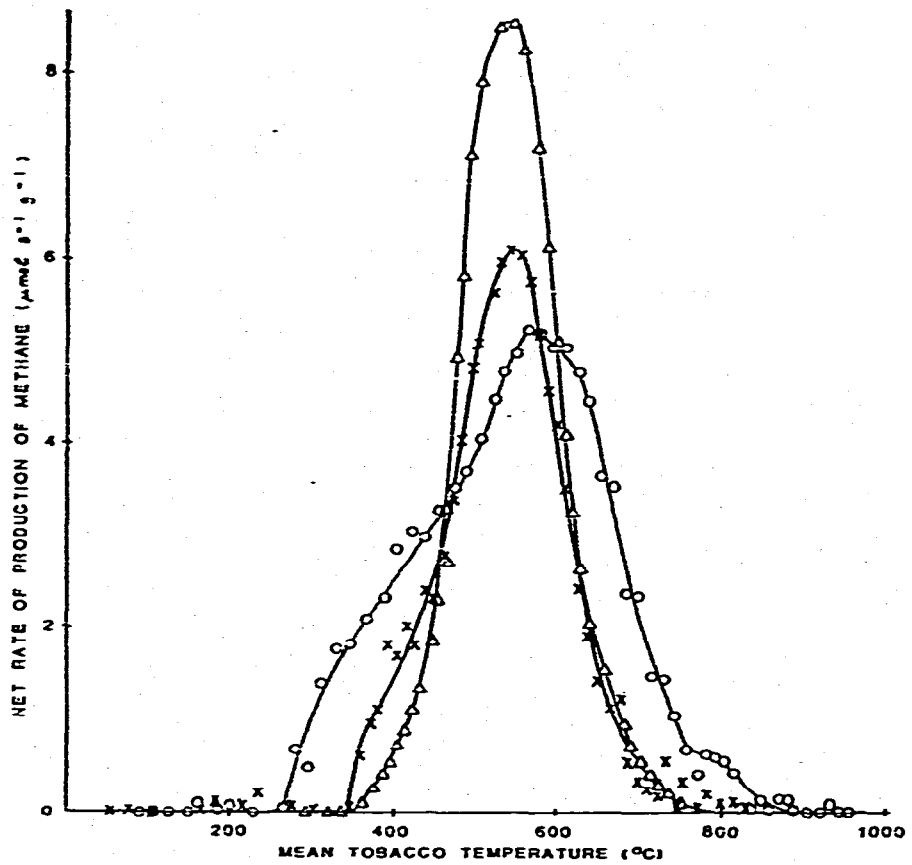

Fig. 10. Effect of oxygen concentration in pyrolysis atmosphere on formation of methane from tobacco pyrolysis. △, Initial $[O_2] = 0$; ×, initial $[O_2] = 9\%$ v/v in nitrogen; ⊙, initial $[O_2] = 21\%$ v/v in nitrogen.

2.2. The effect of homogeneous oxidation of intermediate products

The experiments described in Section 1.1 were repeated, with the tobacco pyrolysed in 9% v/v oxygen in nitrogen. The results obtained for hydrogen, for example, are shown in Fig. 11. The total quantities of products formed are summarised in Table 7. The results are expressed in the experimental units per 0.25 g of tobacco, rather than adjusting them to per gram. This is because the quantities of oxygen used were sufficient to consume the whole of the 0.25 g sample of tobacco used whereas these same quantities would not completely consume 1 g of tobacco (e.g., Fig. 9).

The general trends for methane and propane are the same under both inert and oxidation conditions (Tables 1 and 7)—both have some secondary formation from an intermediate which is not oxidised. However, for the other gases, oxidation in the gas phase is occurring: when the tobacco is placed at the furnace inlet, 8% more oxygen is consumed than at the exit position (Table 7). In the high-temperature region, where oxidation is dominant, the total carbon dioxide produced increases, while the total carbon monoxide decreases, as the residence time of the gases in the furnace increases. Clearly, the effect of the homogeneous combustion of carbon monoxide is

TABLE 6

EFFECT OF PROPORTION OF OXYGEN IN PYROLYSIS ATMOSPHERE ON TOTAL GASES PRODUCED FROM PYROLYSIS OF TOBACCO[a]

Initial conc. of oxygen in pyrolysis gas (% v/v)	*Temp. range (°C)*	*Quantity of individual gases produced (μmol g⁻¹)*							
		H_2	CH_4	C_2H_6	C_3H_8	C_3H_6	CO	CO_2	ΔO_2 (*oxygen consumed*)
0[b]	Low (20–400)			23.6	178		540	2,556	
	High (400–950)			102	275		1,567	852	
	Total (20–950)	2,660	691	125.6	453	46.6	2,107	3,408	—
9[c]	Low (20–400)			35.3	168		522	2,496	619
	High (400–950)			82.8	252		5,081	2,748	4,118
	Total (20–950)	2,000	600	118	420	29.7	5,603	5,244	4,737
21[d]	Low (20–400)				234		782	3,110	1,274
	High (400–950)				321		5,185[e]	5,665	7,212
	Total (20–950)	1,810	535	[f]	555	44.4	5,967	8,775	8,486

[a] 1.0 g of tobacco, pyrolysed in oxygen-nitrogen mixture, inlet flow into furnace = 3.33 cm^3 sec^{-1}. [b] Mean tobacco heating rate = 1.9 K sec^{-1}. [c] Mean tobacco heating rate = 2.1 K sec^{-1}. [d] Mean tobacco heating rate = 2.6 K sec^{-1}. [e] The total quantity of gases figure is obtained from the area underneath the formation rate/time curve. The tobacco heating rate in 21% oxygen is greater than that in 9% oxygen. Consequently, the total amount of carbon monoxide formed between 400–950°C in 21% oxygen is only 2% higher than that formed in 9% oxygen, even though the formation rate of carbon monoxide is higher in 21% oxygen. [f] Figures not available: interference to mass spectrometric peak.

TABLE 7

EFFECT OF POSITION OF TOBACCO IN FURNACE ON TOTAL QUANTITIES OF GASES PRODUCED BY PYROLYSIS IN 9% v/v OXYGEN/91% v/v NITROGEN[a]

Position of tobacco in furnace	*Temp. range (°C)*	*Quantity of individual gases produced (μmol per 0.25 g)*							
		H_2	CH_4	C_2H_6	C_3H_8	C_3H_6	CO	CO_2	ΔO_2 (*oxygen consumed*)
Inlet	Low (20–450)						169	948	
	High (450–900)						957	2,100	
	Total (20–900)	211	156	[b]	167	[b]	1,126	3,048	3,730
Exit	Low (20–450)						148	830	
	High (450–900)						1,165	1,940	
	Total (20–900)	352	143	[b]	146	[b]	1,313	2,770	3,464

[a] 0.25 g of tobacco; inlet flow into furnace = 3.33 cm^3 sec^{-1}, mean tobacco heating rate = 2.1 K sec^{-1}. [b] Formation profiles too ill defined for meaningful integration.

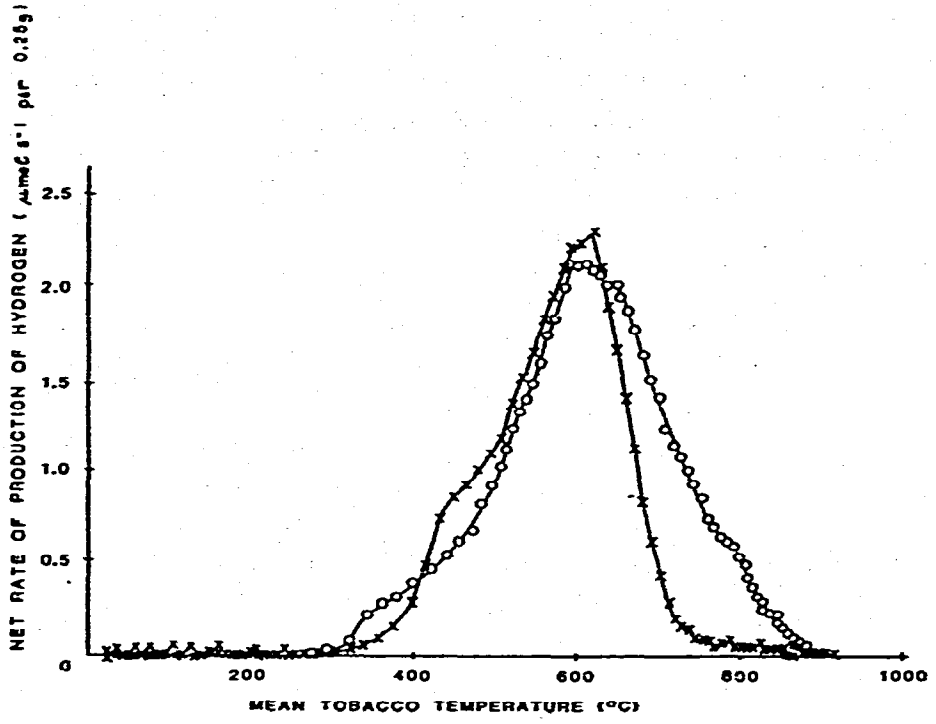

Fig. 11. Effect of varying the residence time of tobacco-pyrolysis products in the furnace on hydrogen formation: tobacco pyrolysed in 9% v/v oxygen in nitrogen. ×, Tobacco at furnace inlet; ⊙, tobacco at furnace outlet.

TABLE 8

PROPORTION (%) OF PRODUCTS FORMED BY HOMOGENEOUS REACTION OF INTERMEDIATE AND FINAL PRODUCTS IN AN OXIDATION ENVIRONMENT

Temp. range (°C)	*Net proportion of product formed, due to homogeneous reaction of intermediate and final products in an oxidation environment*[a]					
	H_2	CH_4	C_3H_8	CO	CO_2	ΔO_2 (*oxygen consumed*)
Low (20–450)				6.6	6.6	
High (450–900)				−9.8	4.0	
Total (20–900)	−25[b]	4.4	6.7	−7.7	4.8	3.7

[a] Proportion $= \dfrac{Q_{inlet} - Q_{exit}}{2\bar{Q}} 100$ (see footnote to Table 2).

where Q_{inlet} = quantity of gases produced with tobacco at inlet position (Table 7); Q_{exit} = quantity ofgases produced with tobacco at exit position (Table 7); and $\bar{Q}$ = mean of Q_{inlet} and Q_{exit}.

[b] Negative quantities indicate that the product has a netconsumption due to homogenous reaction.

greater than the decomposition of intermediates to the carbon oxides. Homogeneous combustion of hydrogen is particularly noticeable (Fig. 11 and Table 7).

At temperatures up to 380°C, the formation rate of carbon dioxide is independent of position in the furnace. This contrasts to the situation in an inert atmosphere where in the same temperature range 5% of the carbon dioxide was formed via intermediate products. These intermediates must either be completely consumed by oxidation reactions, to give products other than carbon dioxide, or their oxidation to carbon dioxide is extremely fast.

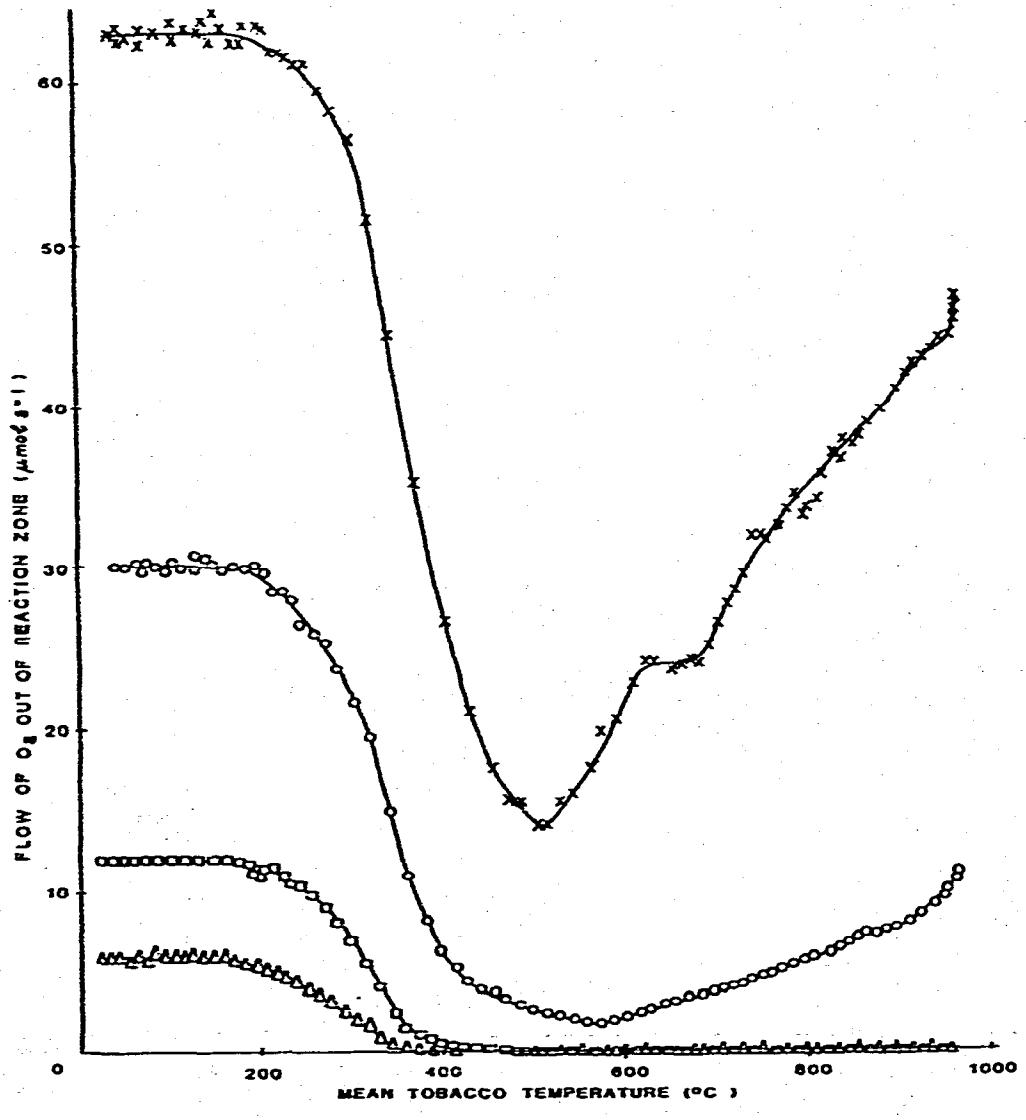

Fig. 12. Effect of gas flow into furnace on resultant flow of oxygen when tobacco is pyrolysed in 9% v/v oxygen in nitrogen. Flow of gas mixture into furnace ($cm^3\ sec^{-1}$): △, 1.67; ⊡, 3.33; ⊙, 8.33; ×, 16.7.

The net proportion of products formed due to homogeneous reaction of intermediate and final products in an oxidation environment is shown in Table 8. Apart from hydrogen, these proportions are small (less than 10%), and their value is determined by the relative proportions of:

(a) formation via homogeneous decomposition of volatile or semi-volatile intermediates,

(b) homogeneous oxidation of the intermediates,

and (c) homogeneous oxidation of the product.

2.3 The effect of space velocity under oxidation conditions

Figures 12 and 13 and Table 9 illustrate the effect of increasing the flow-rate of a 9% v/v oxygen–91% v/v nitrogen gas mixture into the furnace from 1.67 to 16.7 $cm^3\ sec^{-1}$.

In contrast to the situation in an inert atmosphere (Section 1.3), space velocity has a very pronounced effect on the formation rates of the reaction products under oxidation conditions. Because of the exothermicity of the oxidation and the increase in total oxidation with increase in flow-rate, the mean heating rate of the tobacco increases by 35% as the flow-rate into the furnace is increased from 1.67 to 16.7 cm^3

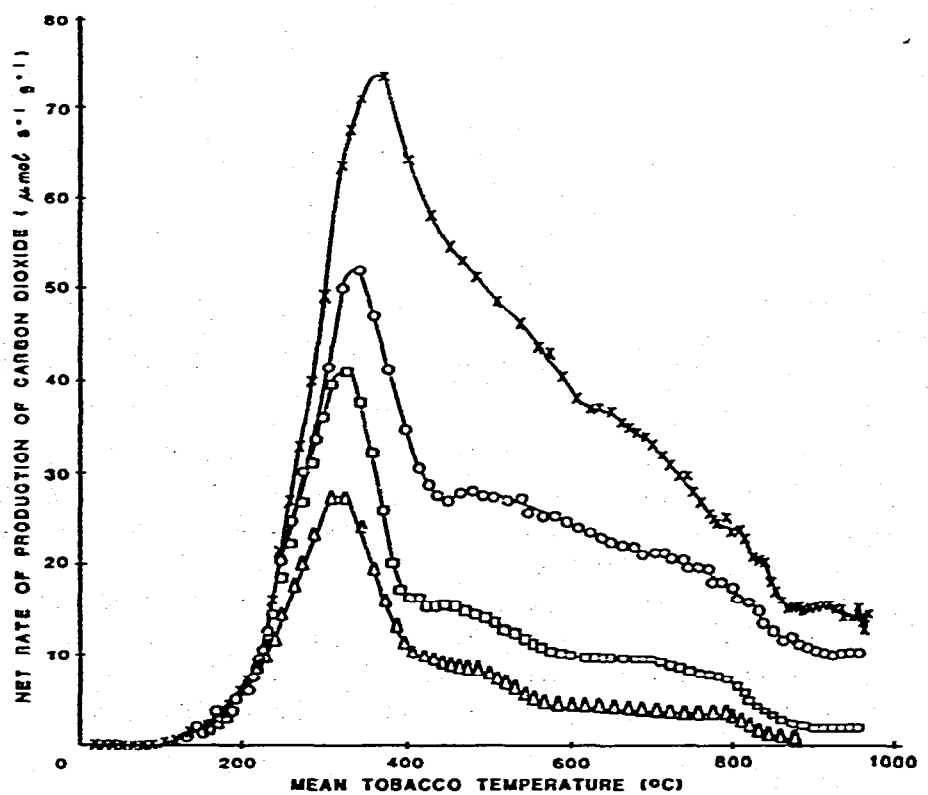

Fig. 13. Effect of gas flow-rate on production of carbon dioxide from tobacco pyrolysis in 9% v/v oxygen in nitrogen. Flow of gas mixture into furnace ($cm^3\ sec^{-1}$): △, 1.67; ⊡, 3.33; ⊙, 8.33; ×, 16.7.

sec^{-1} (see footnote to Table 9). Thus a small proportion of the increase in formation rate with space velocity in Fig. 13, for example, is due to the increased tobacco heating rate*. However, by far the major effect is due directly to the variation in flow velocity itself.

TABLE 9

EFFECT OF GAS FLOW VELOCITY ON TOTAL GASES PRODUCED FROM PYROLYSIS OF TOBACCO IN 9% v/v OXYGEN/91% v/v NITROGEN[a]

Gas flow-rate into furnace ($cm^3\ sec^{-1}$)	*Temp. range* (°C)	*Quantity of individual gases produced* ($\mu mol\ g^{-1}$)							
		H_2	CH_4	C_2H_6	C_3H_8	C_3H_6	CO	CO_2	ΔO_2 (*oxygen consumed*)
1.67[b]	Low (20–450)			10[f]	110[f]		530	2,467	
	High (450–950)			58	228		3,638	1,201	
	Total (20–950)	1,790	620	68	338	28	4,168	3,668	2,340
3.33[c]	Low (20–450)			35.3[f]	168[f]		607	2,929	
	High (450–950)			82.8	252		4,996	2.315	
	Total (20–950)	2 000	600	118	420	30	5,603	5,244	4,740
8.33[d]	Low (20–450)						641	3,152	
	High (450–950)						4,557	4,860	
	Total (20–950)	1,700	530	[g]	550	29[h]	5,198	8,012	7,480
16.7[e]	Low (20–450)						652	3,370	
	High (450–950)						5,286	8,278	
	Total (20–950)	1,812	605	[g]	759	41[h]	5,938	11,648	11,690

[a] 1.0 g of tobacco.
[b] Mean tobacco heating rate = 2.0 K sec^{-1}.
[c] Mean tobacco heating rate = 2.1 K sec^{-1}.
[d] Mean tobacco heating rate = 2.4 K sec^{-1}.
[e] Mean tobacco heating rate = 2.7 K sec^{-1}.
} the differences are caused by the exothermicity of the combustion
[f] 20 to 400°C temperature range. [g] Figures not available: interference to mass spectrometric peak.
[h] Ill-defined profiles.

The oxygen is totally consumed above about 460°C when its input flow $\leqslant 3.33\ cm^3\ sec^{-1}$ (Fig. 12). When its input flow $\geqslant 8.33\ cm^3\ sec^{-1}$, the mass flow of oxygen out of the reaction zone starts to increase at temperatures above 500–600°C, due to consumption of tobacco. Clearly, above 460°C the combustion reaction is controlled by the bulk flow of oxygen into the reaction zone. Further consideration of these results in the next section shows that above about 400°C the reaction rate is limited by the diffusion of oxygen to the surface of tobacco, and that below 400°C both mass transfer and kinetic effects are important in determining the overall reaction rate.

*Using previous data[6], in which the tobacco heating rate was systematically varied, it is estimated that the carbon monoxide and carbon dioxide formation rates would increase by a maximum of 8% due to heating effects, as the flow-rate into the furnace is increased from 1.67 to 16.7 $cm^3\ sec^{-1}$.

Discussion

2.4 Consumption of oxygen: kinetic and diffusion effects

In the present discussion, homogeneous oxidation of intermediate products is ignored, since the results in Table 8 suggest that the effect is kinetically negligible. A generalised reaction scheme for the major products of the combustion (carbon monoxide and carbon dioxide) is given below:

1. $S \rightarrow (CO)_s$
2. $S \rightarrow (CO_2)_s$
15. $S+(O_2)_s \rightarrow (CO)_s$
16. $S+(O_2)_s \rightarrow (CO_2)_s$
17. $(O_2)_g \rightleftharpoons (O_2)_s$
4. $(CO)_s \rightleftharpoons (CO)_g$
5. $(CO_2)_s \rightleftharpoons (CO_2)_g$

The numbering of reaction steps follows in sequence from that used earlier in the paper. Reactions 1 and 2 are tobacco decomposition reactions; reactions 15 and 16 represent generalised reactions of oxygen at the tobacco surface; while steps 17, 4 and 5 represent diffusion processes between the bulk gas phase and the tobacco surface.

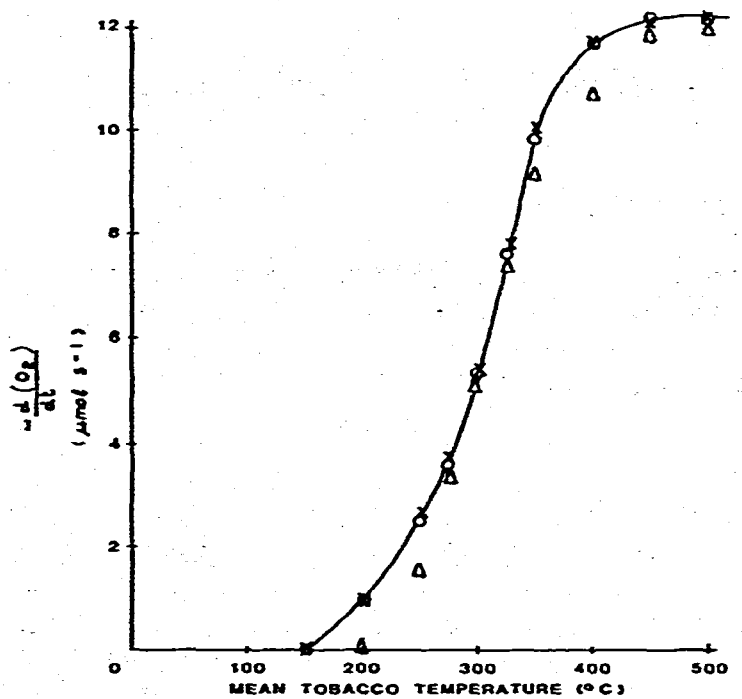

Fig. 14. Rate of consumption of oxygen as a function of tobacco mass, when tobacco is pyrolysed in 9% v/v oxygen–91% v/v nitrogen. ×, 1 g tobacco, centre of furnace; ⊙, 0.25 g tobacco, furnace inlet; Δ, 0.25 g tobacco, furnace exit.

The results in Fig. 14 show that the rate of consumption of oxygen, when tobacco is pyrolysed in 9% v/v oxygen in nitrogen at 2.1 K sec^{-1}, is independent of the mass of tobacco being pyrolysed (0.25–1.0 g), up to 500°C. The data points in Fig. 14 are not extended beyond 500°C because of the excessive consumption of reactant above this temperature for 0.25 g tobacco. Consequently, [S] is relatively large and independent of the quantity of tobacco consumed, so that reaction steps 15 and 16 can be treated as pseudo first-order reactions.

Under stationary or quasi-stationary conditions, the consumption of oxygen at the surface is equal to the rate at which oxygen diffuses to the surface:

$$\frac{\Delta d(O_2)}{dt} = (k_{15}[S]+k_{16}[S])[O_2]_s \tag{26}$$

$$= b_{17}([O_2]_g-[O_2]_s) \tag{27}$$

where b_{17} is the mass transfer coefficient of step 17, given by equations analagous to eqn (2) in Section 1.6.

Substituting the value of $[O_2]_s$ obtained by equating expressions (26) and (27) into expression (26), gives:

$$\frac{\Delta d(O_2)}{dt} = \frac{kb_{17}}{k+b_{17}}[O_2]_g \tag{28}$$

where $k = (k_{15}+k_{16})[S]$ (29)

The bulk concentration of oxygen in the reaction zone, $[O_2]_g$ (μmol cm^{-3}), is given by:

$$[O_2]_g = \frac{\Phi}{F} \tag{30}$$

where Φ is the mean total molar flow of oxygen inside the reaction zone (μmol sec^{-1}) and F is the mean total volumetric gas flow in the reaction zone (cm^3 s^{-1}), given by eqn (7).

The mass transfer coefficient is given by[16]:

$$b_{17} = h_{17}\sqrt{F} \tag{31}$$

where h_{17} is a constant of proportionality.

Thus substituting eqns (30) and (31) into eqn (28), followed by re-arrangement, gives:

$$\frac{R\sqrt{F}}{\Phi} = -\frac{h_{17}}{k}\cdot\frac{RF}{\Phi} + h_{17} \tag{32}$$

where R is equal to $\Delta d(O_2)/dt$.

Data interpolated from Fig. 12 are plotted according to eqn (32) in Fig. 15. The error bars are calculated using the 95% confidence limits of the observed $d(O_2)/dt$

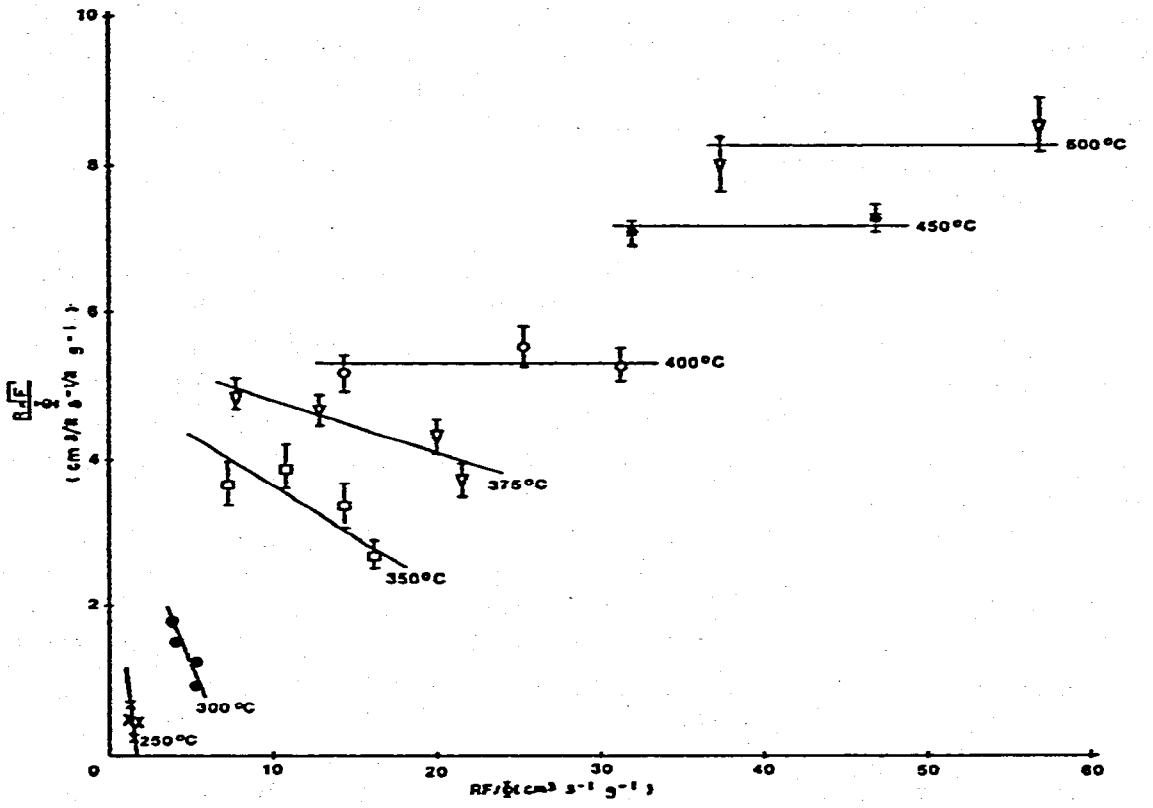

Fig. 15. Pyrolysis of tobacco in 9% v/v oxygen–91% v/v nitrogen: consumption-of-oxygen kinetics

TABLE 10

VALUES OF RATE CONSTANT (k) AND OXYGEN TRANSFER COEFFICIENT (h_{17}) FOR TOBACCO COMBUSTION

Temp. (°C)	k[a] ($cm^3\ sec^{-1}\ g^{-1}$)	h_{17} ($cm^{3/2}\ sec^{-1/2}\ g^{-1}$)
250	1.56	3.20
300	6.86	3.80
350	36.0	5.00
375	78.6	5.50
400	∞[b]	5.30
450	∞	7.16
500	∞	8.26

[a] $k = (k_{15} + k_{16})[S]$

15. $S + (O_2)_s \rightarrow (CO)_s$

16. $S + (O_2)_s \rightarrow (CO_2)_s$

[b] Using the error bars in Fig. 15, the minimum possible value of k at 400°C is 353 $cm^3\ sec^{-1}\ g^{-1}$. A value of ∞ for k indicates that the chemical consumption of oxygen is infinitely fast compared to the diffusion rate of oxygen.

and volumetric flow values. The plots for 450 and 500°C do not include the data points corresponding to inlet flows of 1.67 and 3.33 $cm^3\ sec^{-1}$, since the input oxygen is totally consumed under these conditions (Fig. 12). Plots at temperatures above 500°C are not attempted because of the large consumption of tobacco involved (causing the minima in Fig. 12) invalidating the condition that [S] is large and independent of the quantity of tobacco consumed.

Figure 15 shows that at temperatures above 400°C, the gradients of the plots are zero, indicating that k is infinitely large (eqn (32)). Thus, under these conditions the reaction rate is completely controlled by the bulk phase diffusion of oxygen. Values of h_{17} and k, obtained from the gradient and intercept of the plots in Fig. 15, are given in Table 10. The variation of k with temperature T(K) fits an Arrhenius equation, with an activation energy of 21.4 kcal mol^{-1} and a pre-exponential A factor of $1.49 \times 10^9\ cm^3\ sec^{-1}\ g^{-1}$. The variation of h_{17} with temperature T(K) fits the equation:

$$h_{17} = 6.64 \times 10^{-7} T^{2.46} \tag{33}$$

Theoretically[16], the value of h should be directly proportional to $T^{0.9}$. Thus the above treatment shows that the mass transfer of oxygen in the bulk phase between the tobacco strands is considerably more sensitive to temperature than classical mass transfer theory would suggest. A similar result has been obtained previously, by measuring the diffusion of methane through a tobacco bed by gas chromatography[23], where it was found that the tortuosity factor for methane diffusion through a tobacco bed was proportional to $T^{0.6}$. The extra-temperature dependence probably reflects the continuously changing physical condition of the tobacco with temperature, such as the accessibility of an inner porous structure.

IMPLICATIONS IN A BURNING CIGARETTE

The results presented in Part 2 indicate that at temperatures above 400°C the rate of combustion of tobacco is controlled by the rate of mass transfer of oxygen to the reaction surface. Consequently in the cigarette combustion coal the actual chemical reactions occurring are of secondary importance, the rate of supply of oxygen being the dominant factor in determining the combustion rate and heat generation. Thus cigarettes containing different types of tobacco all have the oxygen concentrations inside their coals reduced to values close to zero, and all have broadly similar temperature distributions. Furthermore, a simplified mathematical expression derived assuming that the diffusion of oxygen is the rate-controlling step in tobacco combustion in a cigarette coal can successfully predict the general shape of the combustion coal[24].

In contrast, the results presented in Part 1 show that the rate of thermal decomposition of tobacco to gaseous products is controlled by the chemical processes involved. Thus, in the region immediately behind the coal, where a large proportion of the products which enter the mainstream smoke are formed, the chemistry of the

tobacco substrate is critical. In addition, the heat release or absorption due to the pyrolytic reactions occurring behind the coal will depend on the chemical composition of the substrate. Thus, together with the differing thermal properties of the tobacco, the temperature gradient behind the coal should depend on the nature of the tobacco.

ACKNOWLEDGEMENTS

The technical assistance of Mr. B. G. Bunn, computing assistance of Mr. J. M. Davey, and the helpful discussions with Dr. K. D. Kilburn are gratefully acknowledged.

REFERENCES

1 J. R. Newsome and C. H. Keith, *Tobacco Sci.*, 9 (1965) 65.
2 R. R. Baker and K. D. Kilburn, *Beitr. Tabakforsch.*, 7 (1973) 79.
3 J. E. Baxter and M. E. Hobbs, *Tobacco Sci.*, 11 (1967) 65.
4 W. R. Johnson, D. H. Powell, R. W. Hale and R. A. Kornfeld, *Chem. Ind.*, (1975) 521.
5 W. P. Pisklov and I. G. Mochnačev, *Ber. Inst. Tabakforsch. (Dresden)*, 18 (1971) 66.
6 R. R. Baker, *Beitr. Tabakforsch.*, 8 (1975) 16.
7 H. R. Burton, *Beitr. Tabakforsch.*, 8 (1975) 78; H. R. Burton and G. Childs Jr., *ibid.*, 8 (1975) 174.
8 W. R. Johnson, R. W. Hale and S. C. Clough, *Nature*, 244 (1973) 51.
9 C. N. Hinshelwood, *The Kinetics of Chemical Change*, Oxford University Press, Oxford, 1955, p. 92.
10 B. W. Wojciechowski and K. J. Laidler, *Trans. Faraday Soc.*, 59 (1963) 369.
11 L. Szirovicza and F. Marta, *Acta Phys. Chem. Szeged*, 18 (1972) 159.
12 D. A. Leathard and J. H. Purnell, *Ann. Rev. Phys. Chem.*, 21 (1970) 197.
13 D. L. Baulch, D. D. Drysdale, D. G. Horne and A. C. Lloyd, *Evaluated Kinetic Data for High Temperature Reactions*, Vol. 2, Butterworths, London, 1973.
14 E. Ratajczak and A. F. Trotman-Dickenson, *Supplementary Tables of Bimolecular Gas Reactions*, UWIST, Cardiff, 1969.
15 C. N. Satterfield, *Mass Transfer in Heterogeneous Catalysis*, M.I.T. Press, Cambridge, Mass., 1970, Ch. 1 and 2.
16 P. L. Walker, Jr., F. Rusinko, Jr. and L. G. Austin, *Adv. Catal.*, 11 (1959) 133.
17 D. A. Frank-Kamenetskii, *Diffusion and Heat Transfer in Chemical Kinetics*, Translation editor J. P. Appleton, Plenum Press, New York and London, 1969, pp. 30 and 34.
18 C. G. von Fredersdorff and M. A. Elliott, H. H. Lowry (Ed.), in *Chemistry of Coal Utilisation*, John Wiley, London and New York, 1963, Supplementary Volume, Ch. 20.
19 S. Ergun and M. Menster, in P. L. Walker, Jr. (Ed.), *Chemistry and Physics of Carbon*, 1 (1965) 203.
20 R. F. Strickland-Constable, *J. Chim. Phys.*, 47 (1950) 356.
21 M. Mentser and S. Ergun, *Carbon*, 5 (1967) 331.
22 R. R. Baldwin, D. Jackson, R. W. Walker and S. J. Webster, Tenth Symposium (International) on Combustion, The Combustion Institute, Pittsburg, Pa., 1965, 423.
23 R. R. Baker, unpublished results.
24 K. Gugan, *Combust. Flame*, 10 (1966) 161.